FP7-600716

Whole-Body Compliant Dynamical Contacts in Cognitive Humanoids

D3.2
Local solver in compliant-world cases

Editor(s)	Vincent Padois[1,2]
Responsible Partner	UPMC
Affiliations	[1] Sorbonne Universités, UPMC Paris 06, UMR 7222, Institut des Systèmes Intelligents et de Robotique (ISIR), F-75005, Paris, France. [2] CNRS, UMR 7222, Institut des Systèmes Intelligents et de Robotique (ISIR), F-75005, Paris, France.
Status-Version:	Final-1.0
Date:	Feb. 28, 2016
EC Distribution:	Consortium
Project Number:	600716
Project Title:	Whole-Body Compliant Dynamical Contacts in Cognitive Humanoids

Title of Deliverable:	Local solver in compliant-world cases
Date of delivery to the EC:	28/2/2016

Workpackage responsible for the Deliverable	WP3
Editor(s):	Vincent Padois
Contributor(s):	Morteza Azzad, Mingxing Liu, Mike Mistry, Francesco Nori, Vincent Padois, Daniele Pucci, Francesco Romano, Silvio Traversaro
Reviewer(s):	
Approved by:	All Partners

Abstract	This deliverable provides an overview of the whole-body control strategies proposed within the framework of the CoDyCo project for balancing by means of compliant contacts. We first recall the general structure of the whole-body controller used in the CoDyCo project. This controller is written as a quadratic multi-objective optimization problem under linear constraints and priorities between the objectives can be dealt with through strict of soft hierarchy. This controller has to be modified in order to deal with compliant cases and two cases are then distinguished. In the first one, a contact model is supposed to be known and using that knowledge a control strategy is derived. In the second case, no model of the environment is assumed to be known and an adaptive force regulation task is added in order to account for the compliance of the environment. This deliverable is strongly related to deliverable 5.3 CITEdeliverable53 which discusses the technical details and choices for the implementation of the year-3 validation scenario.
Keyword List:	Whole-body controllers, Non-rigid contacts, Multi-contacts, Goal-oriented tasks.

Document Revision History

Version	Date	Description	Author
v. 0.1	Jan. 19, 2016	Initial creation of the file	Vincent Padois
v. 0.9	Feb. 25, 2016	Final version	Vincent Padois
v. 1.0	Feb. 28, 2016	Proofread version	Francesco Nori

Table of Contents

Index of Figures

1   Introduction

Under-actuated robots, such as free-floating humanoid robots, usually need to make contacts with their environments to achieve some goal directed whole-body movements. Most researches on whole-body control assume that the environment of the robot is rigid. This means that no adaptation to the environment compliance is needed for controllers. In reality, there is no completely rigid surface even if in practice we can assume a surface to be rigid if it is stiff enough (i.e. deflection is negligible). Unfortunately, many objects in human environments cannot be considered as stiff enough and their compliance has to be accounted for (e.g. a soft cushion, a sofa, a yoga carpet). Indeed, a controller that does not take into account the compliant properties of the contact material may not be sufficient: the compliance of the contact has to be considered by the controller, otherwise the robot may fail to properly balance and fall over. For example, pushing too weakly against a compliant object may not provide the robot with enough reaction forces to support its whole-body tasks. The problem is complex as the rigidity of the object in contact is unknown a priori to robotic controllers, which is usually the case in many scenarios.

The humanoid whole-body control problem has been addressed by different types of whole-body controllers, using analytical approaches [1, 2, 3], constrained quadratic programming [4, 5, 6, 7, 8], or a mixture of them [9, 10]. These controllers are either developed for rigid environments, or validated only in rigid contact scenarios. In general, a valid set of contact forces during whole-body task control can be found by solving a multi-objective problem with a set of elementary task objectives as well as constraints, such as whole-body dynamics, friction cone constraints for non-sliding contacts, and linear complementarity conditions [11, 8, 6, 7], which implies zero relative motions between two bodies in contact when normal contact force is non-negative. In the case of rigid contact with static environment, the linear complementarity condition implies two constraints: (i) the motion of the contact point is zero and (ii) the contact force along the normal to the contact surface is non-negative. The zero motion constraint may not necessarily be true in the case of non-rigid contacts, since the velocities or accelerations of contact points may be non-zero, although the relative motion between the two contact points remains zero. In this case, hybrid control methods [12] that control forces and motions in orthogonal directions are not applicable. Therefore, the controller should take into account the dynamic relation between the contact point position and the contact force, rather than just control the contact force alone.

Such physical interaction dynamics is taken into account in impedance control [13] with the idea of controlling the relation between the contact point motion and the reaction force. Traditional impedance control [13, 14, 15] computes the target impedance of the robot according to the estimated impedance of the environment, which requires high quality measurement of interaction forces. In [16, 17], learning approaches are applied to optimize the robot impedance. Such approaches do not require interaction force sensing and can be adaptable to variable environment impedance. However, the application of such approaches in the context of humanoid balance control with non-rigid contacts is not suitable. First, these methods rely on trajectory-based learning and adaptation algorithms, whereas there is not necessarily a reference motion trajectory for each support contact in the whole-body

balancing context considered here. Furthermore, they need to explore the entire state-action space if a globally optimal solution is to be found, which is impossible for high dimensional robots such as humanoids.

The problem of humanoid balance control with deformable contact support was addressed in [18], which proposed a posture planning approach assuming that the contact material properties are known. Compliant contacts between robots and their environments have been studied by some researchers in other areas such as grasping [19] and animated characters [20]. However, there has not been much research efforts on balancing legged robots on compliant surfaces.

This deliverable provides an overview of the whole-body control strategies proposed within the framework of the CoDyCo project for balancing by means of compliant contacts. It is organized as follows. We first recall the general structure of the whole-body controller used in the CoDyCo project. This controller is written as a quadratic multi-objective optimization problem under linear constraints and priorities between the objectives can be dealt with through strict of soft hierarchy. This controller has to be modified in order to deal with compliant cases and two cases are then distinguished. In the first one, no model of the environment is assumed to be known and an adaptive force regulation task is added to the original "rigid contact" controller in order to account for the compliance of the environment. In the second case, a contact model is supposed to be known and using that knowledge a control strategy is derived.

2   General structure of the whole-body controller in the CoDyCo project

Even though it is not often formulated as such, control of dynamical systems is an optimization problem. Within the framework of the CoDyCo project, the whole-body controller is written as a quadratic multi-objective optimization problem under linear constraints where priorities between the objectives can be dealt with through strict of soft hierarchy. Deliverable 3.1 CITEdeliverable31 exposes the reasons why it is preferable to express controllers in this way. The logic behind this choice can be briefly summarized in a very straightforward way:

1. the equation of motion and joint space to task spaces mappings can be written as equalities but they are not sufficient to describe the overall dynamics and physical behaviour of a robot.

2. Indeed, other intrinsic physical constraint have to be accounted for at the joint level as well as in Cartesian space. These constraints do not solely describe relationships between physical quantities but also limits which cannot (control input saturation) or should never be crossed in order to maintain the robot and its environment in proper working conditions.

3. Theses limits translate into inequalities.

4. Assuming a convex solution space, the optimal solution of the control problem lie at the boundary of the feasible (constraint compliant) solution space.

5. Finding the optimal solution thus boils down to finding the active constraint set, *i.e.* on which boundary it lies.

6. Optimization problem solvers are designed to optimally choose this subset of constraints that should be considered when computing the optimal solution of the control problem.

7. The strong mathematical background in convex optimization is such that optimization based methods mostly outperform analytical methods attempting to heuristically activate constraints.

2.1 Formulation

Based on this formulation choice, the reactive control problem aims at finding at each control instant the actuation torque minimizing $T(\mathbb{X})$, some tasks related function to minimize, given the equation of motion of the multi-body system as well as other equality and inequality constraints. This can be written

$$\tau^* = \underset{\mathbb{X}}{\operatorname{argmin}} \quad T(\mathbb{X}) \tag{1a}$$

$$\text{subject to} \quad M(q)\dot{\nu} + C(q,\nu)\nu + G(q) = B\tau + \underbrace{\sum_{k=1}^{n_c} J_{\mathcal{C}_k}^{\top}(q)f_k}_{J^{\top}(q)f} \tag{1b}$$

$$A(q,\nu)\mathbb{X} = b(q,\nu) \tag{1c}$$

$$D(q,\nu)\mathbb{X} \leq h(q,\nu) \tag{1d}$$

where:

- $\tau \in \mathbb{R}^n$ is the internal actuation torque with $n+1$ the number of rigid bodies – called links – connected by n actuated joints with one degree of freedom each.

- $q \in \mathbb{R}^3 \times SO(3) \times \mathbb{R}^n$ is the generalized coordinates that parametrizes the configuration of the free-floating system. q is a triplet composed of the origin and orientation of the base frame expressed in the inertial frame $\left(^{\mathcal{I}}p_{\mathcal{B}}, ^{\mathcal{I}}R_{\mathcal{B}}\right)$ and the n joint angles q_j.

- $\nu \in \mathbb{R}^{n+6}$ is the system velocity, a triplet concatenating the floating-base twist $\left(^{\mathcal{I}}\dot{p}_{\mathcal{B}}, ^{\mathcal{I}}\omega_{\mathcal{B}}\right)$ and the joint velocities $\dot{q}_j$.

- $J(q) = \begin{bmatrix} J_{\mathcal{C}_1}^{\top}(q) & \dots & J_{\mathcal{C}_k}^{\top}(q) \end{bmatrix}^{\top}$ is the contact Jacobian matrix for all k contact points.

- $f = \begin{bmatrix} f_1^{\top} & \dots & f_k^{\top} \end{bmatrix}^{\top}$ is the vector of external contact wrenches applied by the environment on the links.

- $\mathbb{X} = (\dot{\nu}, \tau, f)$ gathers the dynamic variables of the multi-body system.

- $M \in \mathbb{R}^{n+6 \times n+6}$ is the mass matrix.

- $C \in \mathbb{R}^{n+6 \times n+6}$ is the Coriolis and centrifugal effects matrix.

- $G \in \mathbb{R}^{n+6}$ is the gravity term.

- $B = (0_{n \times 6}, 1_n)^\top$ is a selection matrix.

- $A(q, \nu)\mathbb{X} = b(q, \nu)$ gathers kinematics constraints related to the velocity of the contact points.

- $D(q, \nu)\mathbb{X} \leq h(q, \nu)$ gathers inequality constraints related to joint limits (position and velocity), control input saturation, contact forces (existence and friction limits) and potentially obstacle avoidance.

2.2 Dealing with multiple objectives

The control problem is often multi-objective and the tasks-related function $T((X))$ can actually be written

$$T(\mathbb{X}) = T\left(\lambda_1, T_1(\mathbb{X}), \lambda_2, T_2(\mathbb{X}), \ldots, \lambda_{n_t}, T_{n_t}(\mathbb{X})\right) \tag{2}$$

where $T_i(\mathbb{X})$ is the i-th task among n_t operational tasks to be achieved with $J_i(q)$ its associated task Jacobian and λ_i its priority level. T_i is generally of three types:

- Operational space acceleration $\quad T_i = J_i(q)\dot{\nu} + \dot{J}_i(q_t, \nu)\nu - \ddot{x}^d$
- Joint space acceleration $\qquad\qquad T_i = \dot{\nu} - \dot{\nu}^d$ $\qquad\qquad\qquad$ (3)
- Operational space force $\qquad\qquad T_i = f_{\mathcal{C}_i} - f_{\mathcal{C}_i}^d$

where $\ddot{x}^d$, $\dot{\nu}^d$ and $f_{\mathcal{C}_i}^d$ are desired Cartesian space acceleration, configuration space acceleration and contact wrench respectively, the desired value itself being the outcome of some higher level control architecture (Proportional–Derivative–Integral regulators and/or Momentum regulators and/or Model Predicitve Controllers and/or Trajectory planners providing a feedfoward reference, *etc*).

T_i usually appears in T under the form of a weighted, euclidean norm thus leading to a quadratic cost associated to each task. This quadratic form and the linearity of the constraints allows to resort to the convex optimization techniques, more particularly Linear Quadratic Programs. Then, depending of the type of retained prioritization scheme, the optimization problem 1 can be solved:

1. at once using a single LQP and soft prioritization where T is written as a weighted sum of quadratic costs and where λs play the role of weights for each task, see [21, 22] for examples;

2. using a cascade of LQPs thus inducing strict prioritization between tasks (in that case λs are used to defined a lexicographic order), see [8, 23, 24] for examples;

3. using a representation able to convey both soft and strict prioritization, see [25, 26].

2.3 Direct and two-stage whole-body control approaches

In CoDyCo, these three types of prioritization scheme coexist and are used indifferently as they allow to produce very similar types of behaviours[1]. A distinction has still to be made between two ways to approach the whole-body control problem.

The first, direct, approach does not separate the problem of computing the contact forces from the one of computing the joint torques. Given some task space desired acceleration (among which a center of mass one), the resolution of the control problem described by Equation (1) directly provides the optimal torques. The contact forces come as a by-product of the problem resolution. This approach has the very nice property of being able to account for the joint level constraints. Its drawback is that it hides some of the essence of the balance control problem and while it may be preferable to use such a solution for practical implementation, a two-stage solution may be preferred to ease the analysis of the system (for example in terms of its controllability).

The second, two-stage approach, uses contact forces as intermediate controls and first compute the desired contact forces given the desired acceleration of the center of mass. This can be done using the Newton-Euler equation for the floating-base system, written at the center of mass of the system. It can be written

$$\left(\begin{array}{c} m\ddot{x} \\ \dot{H}_\omega \end{array} \right) = mg + \underbrace{\sum_k \left(\begin{array}{cc} S(p_{\mathcal{C}_k} - x) & 1_3 \\ 1_3 & 0_{3\times3} \end{array} \right) f_k}_{X_{\mathcal{C}}f} \tag{4}$$

where m is the total mass of the system, $x \in \mathbb{R}^3$ is the position of the center of mass expressed in the inertial frame, $\dot{H}_\omega$ is the derivative of the angular momentum, g is the acceleration induced by gravity expressed in the inertial frame, $p_{\mathcal{C}_k}$ is the k-contact point and $S(u) \in \mathbb{R}^{3\times3}$ is the skew-symmetric matrix such that $S(u)v = u \times v$, where $\times$ denotes the cross product operator in $\mathbb{R}^3$.

Equation (4) plainly displays the relation between contact wrenches and the dynamics of the center of mass and f can be computed based on it in order to achieve some desired center of mass linear acceleration $\ddot{x}^d$ and to maintain the angular momentum null (by choosing $\dot{H}_\omega = 0$). The solution for f can be computed using an LQP as well. This allows to account for inequality constraints related to friction. Given these desired contact forces, the whole-body control problem can then be solved using the general formulation provided by Equation (1). This control approach, often referred as *momentum-based balance controller*, has extensively been used in the recent years [27, 28, 29] and is the one used in the CoDyCo demonstrations.

The next sections describe how this generic controller structure can be exploited and adapted to deal with compliant contacts.

---

[1]A formal comparison of their intrinsic properties is out of the scope of this deliverable but would constitute a work of interest for the community
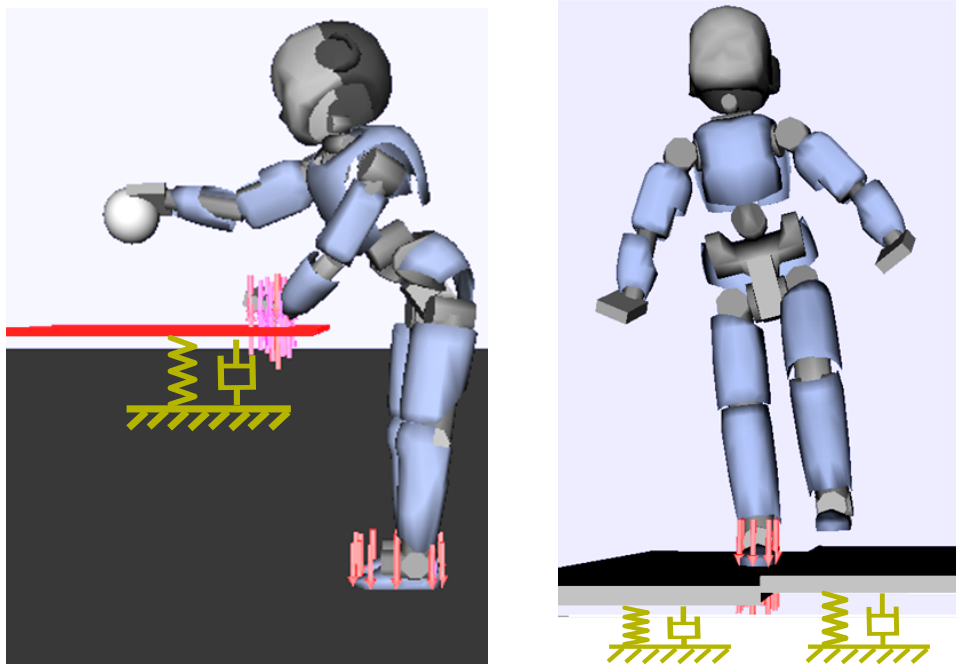
Figure 1: Examples of balancing on non-rigid contacts during whole-body task execution.

3 Balancing on compliant contacts: model-free control approach

When robots evolve in partially known environments, model-based control approaches requires to incrementally, through experience, modify existing models or build new ones (see CITEdeliverable4.2 for details on learning of tasks with multiple contacts by imitation and reinforcement learning). While models evolve, the robot still needs to be able to act accordingly, or at least without failure, in this, partially known, environment. Providing an adaptive control approach, not relying on a compliance model, in order to adapt the whole-body motions of humanoid robots to unknown rigidity properties of the environment is thus of interest.

3.1 Summary of the contribution

The work described hereafter was published in [30] and is dedicated to whole-body balancing, and more generally whole-body control, with non-rigid, unilateral, frictional support contacts, for example, standing on a soft ground, or pushing against a compliant support contact with one hand while reaching for an object far away with the other hand (see Fig.1). The problems of the manipulation of compliant objects and the handling of unexpected disturbance forces are beyond the scope of this work. Moreover, the proposed control approach does not handle anticipatory aspects of balance, but it provides a reactive mechanism to maintain balance while multiple motion and contact tasks are being performed in a compliant environment.

The contribution of this work consists in a reactive controller for whole-body balancing of humanoid robots performing whole-body tasks in unknown compliant environments. As the motions and forces at support contacts are related to whole-body task executions,

their reference trajectories are unavailable a priori. Therefore, this approach focuses on the regulation of contact forces in a reactive way. It reacts to the motions of non-rigid contacts in real-time during whole-body movements, with the aim of establishing contact equilibrium quickly.

A frictional non-rigid contact model is proposed both for simulation and for control. The model parameters of the non-rigid environment are unknown to the controller. The force regulation approach does not try to estimate the impedance parameters of the environment, but it regulates contact forces by reacting to environment motions directly. This reactive control approach is embedded in an optimization based multi-task controller of type (1), which has been used to achieve whole-body control of humanoid robots in rigid environments. However, the reactive principle of the approach proposed here is general and can also be applied in many other whole-body controllers to handle non-rigid support contacts. Examples using this approach are provided, where a humanoid robot performs reaching and stepping actions in a non-rigid environment. Further research directions related to this approach are also presented. Details can be found in the paper hereafter included.

3.2 Reactive whole-body control for humanoid balancing on non-rigid unilateral contacts

Reactive whole-body control for humanoid balancing on non-rigid unilateral contacts

Mingxing Liu and Vincent Padois

Abstract— **Humanoid robots are expected to act in human environments, where some of the contacts can be non-rigid. A fairly large amount of work has been devoted to the whole-body control of humanoids under rigid contacts, but few of them take into account non-rigid contacts. Indeed, the handling of unknown compliant contacts to achieve goal directed actions and whole-body balance remains a challenge. This paper addresses this problem by proposing a control mechanism that solves whole-body tasks under non-rigid contacts. It is a reactive control approach that automatically regulates contact forces and whole-body motions based on the motion of contact points without the awareness of the rigidity properties of the contact material. Verification of this approach is conducted through experiments on the iCub humanoid robot in simulation.**

I. INTRODUCTION

Under-actuated robots, such as free-floating humanoid robots, usually need to make contacts with their environments to achieve some goal directed whole-body movements. Most researches on whole-body control assume that the environment of a robot is rigid. This means that no adaptation to the environment compliance is needed for controllers. However, many objects in human environment can be compliant (e.g. a soft cushion, a sofa, a yoga carpet). In this case, a controller that does not take into account the rigidity properties of the contact material is not sufficient. For example, pushing too strongly against a rigid object may result in damages to the robot or the environment; and pushing too weakly against a compliant object may not provide the robot with enough reaction forces to support its whole-body tasks. The problem becomes more complex when the rigidity of the object in contact is unknown a priori to robotic controllers, which is usually the case in many scenarios.

This paper aims at adapting whole-body motions of humanoid robots to unknown rigidity properties of the environment. This work is dedicated to whole-body balancing, and more generally whole-body control, with non-rigid, unilateral, frictional support contacts, for example, standing on a soft ground, or pushing against a compliant support contact with one hand while reaching for an object far away with the other hand (see Fig.1). The problems of the manipulation of compliant objects and the handling of unexpected disturbance forces are beyond the scope of this paper. Moreover, the proposed control approach does

The authors are with

-Sorbonne Université, UPMC Univ Paris 06, UMR 7222, Institut des Systèmes Intelligents et de Robotique, F-75005, Paris, France

-CNRS Centre National de la Recherche Scientifique, UMR 7222, Institut des Systèmes Intelligents et de Robotique, F-75005, Paris, France
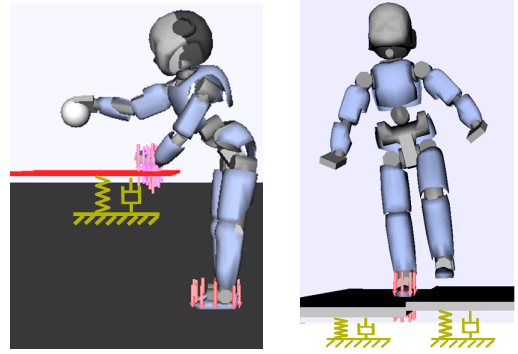
`{liu, padois}@isir.upmc.fr`

Fig. 1. Examples of balancing on non-rigid contacts during whole-body task execution.

not handle anticipatory aspects of balance, but it provides a reactive mechanism to maintain balance while multiple motion and contact tasks are being performed in a compliant environment.

A. Related work

The humanoid whole-body control problem has been addressed by different types of whole-body controllers, using analytical approaches [1]–[3], constrained quadratic programming [4]–[7], or a mixture of them [8,9]. These controllers are either developed for rigid environments, or validated only in rigid contact scenarios. In general, a valid set of contact forces during whole-body task control can be found by solving a multi-objective problem with a set of elementary task objectives as well as constraints, such as whole-body dynamics, friction cone constraints for non-sliding contacts, and linear complementarity conditions [6,7,10], which implies zero relative motions between two bodies in contact when normal contact force is non-negative. In the case of rigid contact with static environment, the linear complementarity condition implies two constraints: (i) the motion of the contact point is zero and (ii) the contact force along the normal to the contact surface is non-negative. The zero motion constraint may not necessarily be true in the case of non-rigid contacts, since the velocities or accelerations of contact points may be non-zero, although the relative motion between the two contact points remains zero. In this case, hybrid control methods [11] that control forces and motions in orthogonal directions are not applicable. Therefore, the controller should take into account the dynamic relation between the contact point position and the contact force, rather than just control the contact force alone.

Such physical interaction dynamics is taken into account in impedance control [12] with the idea of controlling the relation between the contact point motion and the reaction force. Traditional impedance control [12]–[14] computes the target impedance of the robot according to the estimated impedance of the environment, which requires high quality measurement of interaction forces. In [15,16], learning approaches are applied to optimize the robot impedance. Such approaches do not require interaction force sensing and can be adaptable to variable environment impedance. However, the application of such approaches in the context of humanoid balance control with non-rigid contacts is not suitable. First, these methods rely on trajectory-based learning and adaptation algorithms, whereas there is not necessarily a reference motion trajectory for each support contact in the whole-body balancing context considered here. Furthermore, they need to explore the entire state-action space if a globally optimal solution is to be found, which is impossible for high dimensional robots such as humanoids.

The problem of humanoid balance control with deformable contact support was addressed in [17], which proposed a posture planning approach assuming that the contact material properties are known. A difference of the present paper with respect to [17] is that the approach proposed here does not require the knowledge of the rigidity of the environment, and the controller works online in a reactive way.

B. Contribution

The contribution of this work consists in a reactive controller for whole-body balancing of humanoid robots performing whole-body tasks in unknown compliant environments. As the motions and forces at support contacts are related to whole-body task executions, their reference trajectories are unavailable a priori. Therefore, this approach focuses on the regulation of contact forces in a reactive way. It reacts to the motions of non-rigid contacts in real-time during whole-body movements, with the aim of establishing contact equilibrium quickly.

A frictional non-rigid contact model is proposed (Section II) both for simulation and for control. The model parameters of the non-rigid environment are unknown to the controller. The force regulation approach does not try to estimate the impedance parameters of the environment, but it regulates contact forces by reacting to environment motions directly. This reactive control approach is embedded in an optimization based multi-task controller (Section III), which has been used to achieve whole-body control of humanoid robots in rigid environments. However, the reactive principle of the approach proposed here is general and can also be applied in many other whole-body controllers to handle non-rigid support contacts. Examples using this approach are provided in Section IV, where a humanoid robot performs reaching and stepping actions in a non-rigid environment. Further research directions related to this approach are presented in Section V.
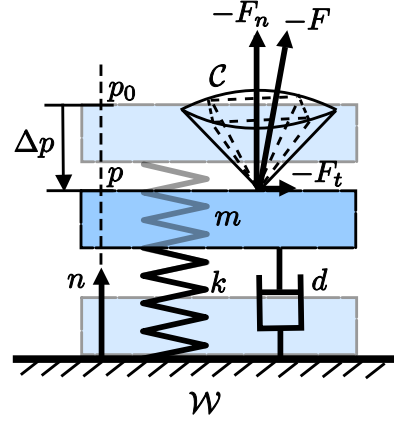

Fig. 2. Modeling of a frictional non-rigid contact with a mass spring damper system and Coulomb's friction cone.

II. CONTACT MODELING

This work considers the handling of non-rigid support contacts. The environment is assumed to be passive and the contact surface at each contact point is supposed to be flat. The direction perpendicular to the contact surface and pointing towards the robot is denoted by n. The interaction force exerted by the robot on the environment is $F = [F_t^T, F_n^T]^T$, with F_t, the tangential contact force and $F_n = -F_n n$, the normal force (the component perpendicular to the contact surface).

The dynamics of a non-rigid environment here is modeled as a mass-spring-damper system as shown in Fig. 2. A rigid mass is attached to a massless spring with spring constant k and a massless viscous damper with constant d. In the model used here, the mass only moves along the directions n or $-n$. The position of the contact point along n is denoted as $p = pn$. The normal velocity of the contact point with respect to the world frame $\mathcal{W}$ is denoted as v_n. The length of the spring is limited. When the spring is not completely compressed, the magnitude of the normal contact force exerted by the robot on the environment is

$$F_n = m\ddot{p} + k\Delta p + d\dot{p}, \text{ with } \|\Delta p\| \leq \Delta p_{max} \quad (1)$$

where $\Delta p = p - p_0$ is the displacement of the mass with respect to its rest position p_0, and Δp_{max} is the limit amount of the displacement. When the spring is completely compressed, the contact becomes rigid. For the contact to exist, the normal contact force must be non-negative: $F_n \geq 0$, because the contact point of the robot can only push the mass but not pull it (unilateral contact).

To ensure a non-sliding contact, the frictional contact force is constrained to lie within the Coulomb friction cone: $\mathcal{C} = \{F \mid \|F_t\| \leq \mu \|F_n\|\}$, where $\mu > 0$ is the friction coefficient at the contact point. The friction cone is usually approximated by a *k*-faced convex polyhedron so that the non-sliding contact constraint can be formulated as a linear constraint.

III. Reactive Whole-Body Control under Non-Rigid Contacts

The reactive whole-body control proposed here solves a set of elementary operational tasks as well as constraints to ensure whole-body balance during task execution. An elementary operational task considered here can be either a motion task (e.g. center of mass motion task, hand motion task, foot motion task, posture task, etc.), or a contact task (hand contact task, foot contact task, etc.). Especially, the above-mentioned contact model is used here to adapt whole-body movements to frictional non-rigid support contacts. The whole-body control of all the tasks and constraints are formulated as a Linear Quadratic Programming (LQP) problem (2). The output of this LQP problem is the optimal joint accelerations $\ddot{q}$, joint torques τ, and contact forces F.

$$\underset{\ddot{q},\tau,F_c}{\arg\min} \quad \sum_i \left\| J_i(q)\ddot{q} + \dot{J}_i(q)\dot{q} - \ddot{p}_i^d \right\|_{Q_i}^2 \tag{2a}$$

$$+ \sum_c \left\| F_c - F_c^d \right\|_{Q_c}^2 \tag{2b}$$

$$+ \|\tau\|_{Q_r}^2 + \|\ddot{q}\|_{Q_r}^2 \tag{2c}$$

$$\text{s.t.} \quad M(q)\ddot{q} + b(q,\dot{q}) = S^T\tau - \sum_c J_c(q)^T F_c \tag{2d}$$

$$F_c \in \mathcal{C}_c \tag{2e}$$

$$\underline{F_c} \le F_c \le \overline{F_c} \tag{2f}$$

$$\underline{\tau} \le \tau \le \overline{\tau} \tag{2g}$$

$$\underline{q} \le \tfrac{1}{2}\ddot{q}\delta t^2 + \dot{q}\delta t + q \le \overline{q} \tag{2h}$$

where several task objectives are optimized subject to the whole-body dynamics constraint (2d), the friction cone constraint (2e), bounds on contact forces (2f), joint torque limits (2g), and joint limits (2h). $M(q)$ is the generalized inertia matrix. $\dot{q}$ and $\ddot{q}$ are the vector of velocity and the vector of acceleration in generalized coordinates, respectively. $b(q,\dot{q})$ is the vector of Coriolis, centrifugal and gravity induced joint torques. S is a selection matrix for the actuated degrees of freedom (DoF). Joint limit constraint (2h) is expressed with respect to joint accelerations based on a discrete linear approximation of joint positions with a time step of δt.

Objective (2a) minimizes the error of task acceleration for elementary motion task control. Each motion task i is associated with a local proportional-derivative (PD) controller $\ddot{p}_i^d = K_{p,i}e_i + K_{d,i}\dot{e}_i$. The inputs of this PD controller are task position and velocity errors (e_i and $\dot{e}_i$), and the output is the desired acceleration $\ddot{p}_i^d$ of the controlled frame. Here $K_{p,i}$ and $K_{d,i}$ are symmetric, positive definite gain matrices, J_i is the task Jacobian, and Q_i is a diagonal weighting matrix to regulate the importance level of task i.

As the contact force F_c affects the whole-body motion, its appropriate value should be computed in consideration of all the tasks to be performed and constraints to be met. There are actually infinite contact force solutions that satisfy all these task objectives and constraints. The regularization task (2b) can be used to ensure the uniqueness of the solution by mimizing the norm of F_c. Indeed, as mentioned in [5],
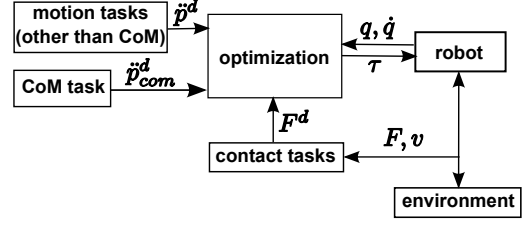

Fig. 3. Block schema of the whole reactive whole-body control system.

one can set the value of desired contact force F_c^d in (2) to zero, set the weight Q_c to a low value compared to Q_i, and let the optimization to compute the appropriate value of F_c. However, in this work, which deals with non-rigid contacts, F_c^d is computed according to the local contact information, in order to speed up robot reaction to non-rigid contacts. This computation of F_c^d is described in III-A. This desired contact force is used to guide the search of the optimal contact force in optimization (2), and the suitable value of F_c is still provided by (2) to satisfy all the constraints in (2).

Objective (2c) is a regulation term that minimizes the norms of the variables τ and $\ddot{q}$. This objective is useful for ensuring the uniqueness of the solution for redundant robots. As this objective may increase the errors of other elementary tasks, its weight Q_r is set to a very low value compared to other objective weights. The whole reactive whole-body control system is summarized in Fig. 3.

A. Handling of interaction force at non-rigid support contact

In this work, a multi-contact state is supposed to be in static equilibrium if there is no motion at support contacts. Take the reaching scenario shown in Fig. 1 for example, if the support hand pushes too slightly against the table surface, the reaction force generated by the table is too weak to support the robot's leaning posture, and the robot may not be able to provide enough joint torques to maintain its posture. In this case, the contact is not in equilibrium as the support hand will keep sinking with the table surface. If the hand pushes strongly enough, the contact equilibrium may be established. However, the multi-contact system usually does not have a unique equilibrium state due to the redundancy of the system. In the reaching scenario, three situations can be listed when the robot leans forward to reach for an object:

1) if the hand contact force is weak, the robot may have to strengthen a lot in order to maintain the leaning posture.
2) If the hand pushes the table more strongly, a sufficient reaction force is generated by the supporting surface to maintain the leaning posture, and the robot does not have to strength a lot to maintain contact equilibrium.
3) If the hand pushes the table too strongly, the robot may have to strengthen a lot again in order to balance internal forces created by hand contact force to maintain equilibrium.

As there is a wide range of hand contact forces that can satisfy the equilibrium of the multi-contact system, it is

desirable to find appropriate contact forces to rapidly achieve an equilibrium state in a natural way. Therefore, in addition to the optimization of contact forces by a comprehensive consideration of all the task objectives and constraints in (2), the desired contact force is adapted to local contact information. Indeed, as long as the contact point is moving along the pushing direction, the robot cannot rely on this contact point to maintain its equilibrium and the desired contact force will be kept increased until the material is sufficiently compressed and no more movement is produced at the contact point ($v_c = 0$). In this way, the contact equilibrium is attained rapidly and the contact point can fully support the whole-body task execution.

The regulation of the desired contact force depends on the rigidity of contact materials. Although the contact material is unknown a priori, the robot can adapt its rigidity by pushing against it. Here the approach does not estimate the parameters of a model of the environment, but it does regulate the contact force in a reactive way. The idea is to first apply a small amount of pushing force $\underline{F}_c$ at the beginning of contact ($F_c^d(t_0) = \underline{F}_c$) to activate it. If the contact surface is soft, then it starts to move along the pushing direction ($v_c > 0$). Afterward, the variation of desired contact force δF_c is computed at each time step during the pushing action.

The form of δF_c can be chosen by an analysis of the energy variation during the pushing action[1]. At time $t = t_l$, the kinetic energy of the local interaction system is $\frac{1}{2}m_c(t_l)\|v_c(t_l)\|^2$, where m_c is the equivalent mass of the robot-environment system at contact point c. Part of this energy is supposed to be absorbed by the spring displacement Δp, with the rest being dissipated by the damper after a short amount of time Δt

$$\frac{1}{2}k\Delta p^2 + \int_{t_l}^{t_l+\Delta t} d\|v_c(t)\|^2\,\mathrm{d}t = \frac{1}{2}m_c(t_l)\|v_c(t_l)\|^2. \quad (3)$$

Substituting the total variation of the spring force from t_l to the end of pushing $\Delta F_c = k\Delta p$ in (3) leads to

$$\|\Delta F_c\| = \frac{m_c(t_l)\|v_c(t_l)\|^2 - 2\int_{t_l}^{t_l+\Delta t} d\|v_c(t)\|^2\,\mathrm{d}t}{\|v_c(t_l)\|\,\Delta t}. \quad (4)$$

Supposing v_c is constant from t_l to $t_l + \Delta t$, the order of magnitude of $\|\Delta F_c\|$ can be estimated to be $\left(\frac{m_c(t_l)}{\Delta t} - 2d\right)\|v_c(t_l)\|$. This extra amount of spring force needs to be balanced by extra robot contact forces finally to maintain contact equilibrium. In fact, the increase of the contact force at each time step may result in the increase of the contact point velocity towards the pushing direction, thus it may accelerate the pushing action until the material is completely compressed with respect to the whole-body motion of the robot. Based on the above analysis, the desired contact force variation can have the same order of magnitude as ΔF_c does, which is proportional to $v_c(t_l)$. Therefore, the

---

[1]It is assumed here that the impedance of the robot itself remains high with respect to the impedance of the contact surface and that the energy is mostly dissipated by the non-rigid environment.

desired contact force $F_c^d(t_l)$ can be computed as follows

$$\begin{aligned} F_c^d(t_l) &= F_c(t_{l-1}) + \delta F_c(t_l) \\ \text{with } \delta F_c(t_l) &= a(t_l)v_c(t_l), \end{aligned} \quad (5)$$

where $a(t_l)$ is a non-negative parameter. A large value of a corresponds to a small value of Δt, which implies a faster pushing action. To avoid abrupt changes in the contact force, the value of δF_c is bounded. Moreover, for safety reason, the contact force is limited by its upper bound $\overline{F_c}$ in (2f) to prevent the robot from pushing too strongly when it touches a very rigid surface at the end of the pushing action.

B. Center of mass control

During a quasi-static movement, the position of center of mass (CoM) plays an important role in balance control. For fixed contact point placements, the CoM must lie above the projection of a convex set that is defined by the properties of each contact placement [18]. In many applications, the CoM target position is given a priori. For example, it is usually fixed above the center of support polygon when the robot is standing, or planned by predictive control for locomotion [19]. Moreover, the CoM task is usually assigned with a high priority with respect to contact force related tasks (not contact constraints) to ensure balance. In this case, the CoM position may dominate the control of contact forces. For example, no matter what desired contact force is assigned to a foot contact task of a standing robot, its real value will be governed by the motion of the CoM. However, the desired CoM position planned a priori may not be suitable in a non-rigid environment, because the planner cannot take into account the unknown rigidity of the contact surface. Therefore, the planned CoM target position is adjusted here to adapt to the compliance of the environment, or in other words, to the desired contact forces at non-rigid support contacts.

The adaptation of the CoM position is based on a simplified model of the robot, including a punctual mass (m) at the CoM linked to several massless legs or arms. This simplified model is in static equilibrium under desired contact forces F_c^d if

$$\sum_c F_c^d + mg = 0 \quad (6a)$$

$$\sum_c p_c \times F_c^d + p_{com} \times mg = 0 \quad (6b)$$

$$F_c \in \mathcal{C}_c, \quad (6c)$$

where F_c^d is computed in (5), g is gravity acceleration, p_c is the position of contact point c, and p_{com} is the CoM position. Condition (6c) is momentarily neglected here since it is accounted for when solving (2). The other two conditions (6a) and (6b) allow us to compute p_{com}^d compatible with F_c^d by solving

$$\sum_c p_c \times F_c^d - p_{com}^d \times \sum_c F_c^d = 0. \quad (7)$$

It can be proved that the components of p_{com}^d in the plane of contact surface can always be found by solving (7), as long as
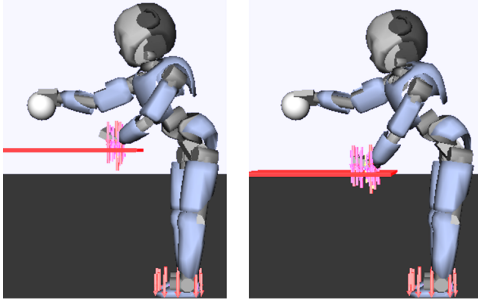
Fig. 4. Snapshots of the robot reaching with one hand supported by a table. The table on the right is softer than the one on the left.
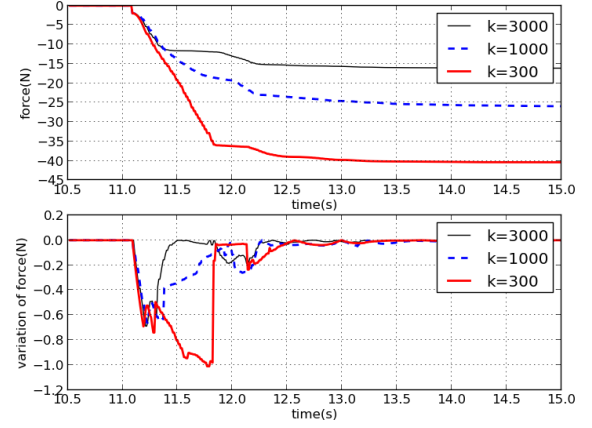

Fig. 5. The contact force between the left hand and the table (above) and the variation of desired contact force (below). The stiffness of the table is modified, from $k = 300N/m$ to $k = 3000N/m$, the contact point displacement is limited by $\Delta p_{max} = 5cm$, and d is set to $2\sqrt{k}$.
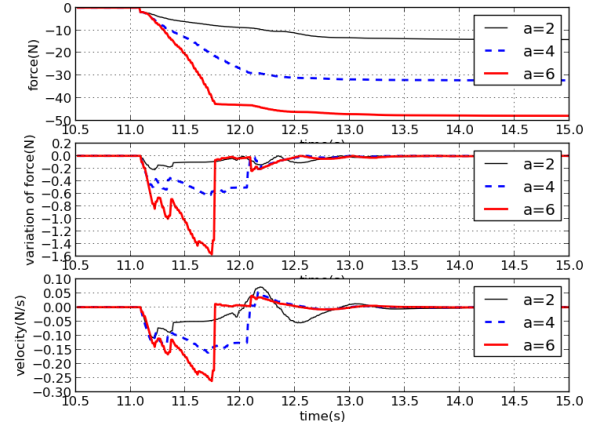

Fig. 6. The contact force between the left hand and the table (above), the variation of desired contact force (middle), and the hand velocity (below). The stiffness of the table is $k = 300N/m$, and a is changed from $2Ns/m$ to $6Ns/m$. A larger a results in stronger contact force, but establishes contact equilibrium faster; while a smaller a provides weaker support force, resulting in more fluctuation of velocity during whole-body task execution.

the contact forces along the normal direction are constrained to be non-zero, which can be ensured by setting $\underline{\boldsymbol{F}_c} > \boldsymbol{0}$ in (2f). Note that $\boldsymbol{p}_{com}^d$ is computed to be adaptable to $\boldsymbol{F}_c^d$ but with (6c) neglected. Therefore, to ensure equilibrium for the robot, the adapted CoM target position $\boldsymbol{p}_{com}^d$ should be further constrained within its admissible domain defined by (6), which can be obtained by using the approach described in [18].

IV. RESULTS

The reactive whole-body control proposed in section III is applied here to handle multiple non-rigid contacts during whole-body task execution. The approach is applied to a 38-DoF free-floating iCub robot in the simulator XDE [20], which is a software environment that manages physics realistic simulation. Some example applications of the proposed approach can be seen in the video attached to this paper. These applications are: reaching with one hand supported by tables of different degrees of rigidity and stepping on a soft floor.

A. Reaching with one hand supported by a soft table

In this scenario, the robot is standing on the ground and reaching for an object above a table with its right hand. As the object is far away, its left hand is in contact with the table to obtain an additional support that increases its reaching ability (see Fig. 4). The non-rigid table is modeled using the model described in II. The controlled motion tasks include the 2-D CoM position task, 6-D the right hand position and orientation task, the 32-D posture task, and the 1-D head position task. The right hand target position is the object above the table. The posture task tries to keep the body upright. The contact tasks handle the left hand contact with the table and eight foot contacts with the ground. Each contact force is constrained to lie inside a friction cone to avoid slippage. The maximum magnitudes of the hand contact force $\overline{\boldsymbol{F}_c}$ and of its variation $\overline{\delta\boldsymbol{F}_c}$ are set to $50N$ and $1.5N$, respectively. The minimum contact force $\underline{\boldsymbol{F}_c}$ is set to $2N$ to keep the contact active.

In this experiment, different degrees of rigidity of the table are tested, from a very soft case to a nearly rigid case. In all these tests, the robot is able to adapt the pushing behavior of the left hand, and the right hand successfully

reaches the goal. The resulting hand contact force ($\boldsymbol{F}_c$) as well as its desired variation ($\delta\boldsymbol{F}_c$) is shown in Fig. 5, with the coefficient a set to $5Ns/m$.

This figure shows that the hand contact force converges no matter if the table surface is soft ($k = 300N/m$) or hard ($k = 3000N/m$). When the table is soft, larger force variations are generated during the pushing action in order to establish contact equilibrium quickly. The softer the table is, the stronger the resulting contact force becomes. This is logical since the soft table displaces easily while being pushed, so that the hand sinks together with the table, making the body lean forward more. Thus more reaction force is needed from the table to support the bended posture.

The role of a is to regulate the ratio of force variation with

respect to contact point velocity. In Fig. 6, contact forces as well as contact point velocity with respect to different values of a and the same table stiffness ($k = 300N/m$) are shown. It can be seen that a larger a makes the contact point sinks faster, resulting in stronger contact force, but making the velocity converges to zero faster; while a smaller a provides weaker support force, resulting in more fluctuation of velocity during whole-body task execution. The choice of the value of a depends on how quickly the equilibrium is desired to be established. However, a too large a may result in too large force variation. Therefore, the magnitude of the force variation is bounded here to avoid large peaks in contact forces.

The computation time for the proposed control algorithm for this experiment is presented in Figure 7. It can be seen

Fig. 8. Snapshots of the robot stepping on a soft floor.

Fig. 9. The contact forces on left foot (lf) and right foot (rf) (above), the variations of desired foot contact forces (middle), and the positions of CoM and the feet (below). The stiffness of the floor is $k = 1000N/m$, and a is set to $10Ns/m$.
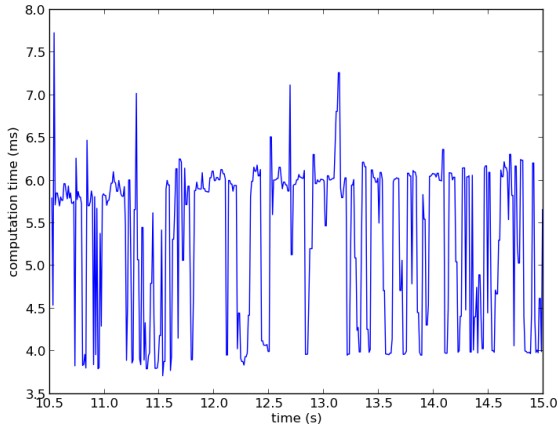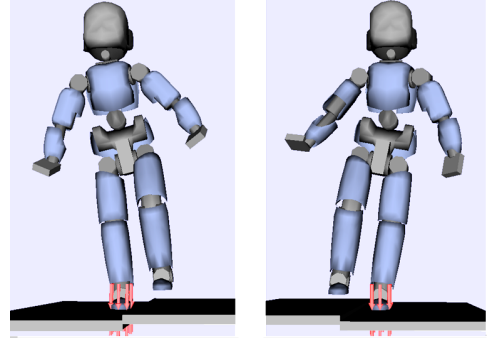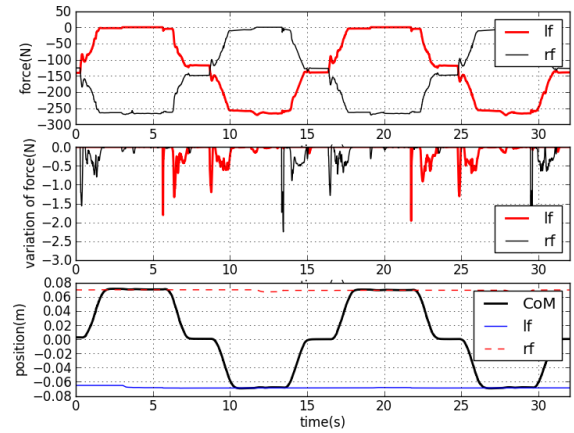

Fig. 7. Computation time for the control algorithm.

in Figure 7 that for the iCub robot with 38 DoF performing 13 motion and force tasks, and with a total task dimension of 68, the computation time for the control algorithm is within $10ms$ without any specific code optimization. Real time implementation of the proposed approach on a torque controlled humanoid robot can thus be envisioned.

B. Stepping on a soft floor

In this experiment, the robot keeps switching its stance foot on a soft floor (see Fig. 8). The soft floor is modeled as two separate movable planks, one under each foot. The controlled tasks include the CoM task, the moving foot task, the posture task, and the stance foot contact task. Each foot contact force is constrained to lie inside a friction cone to avoid foot slippage. As mentioned in section III-B, instead of manually switching the CoM target position between above the two feet, it is computed automatically based on the desired foot contact force by solving (7).

The resulting foot contact forces and the profile of the CoM position are shown in Fig. 9. Here the CoM reference position is computed according to foot positions and desired foot contact forces. One can obtain similar results by first defining the CoM reference trajectory, and then let controller

(2) to find appropriate foot contact forces without adaptation to ground rigidity. This is because for a humanoid robot which is a biped, there is not much contact redundancy, and the position of the CoM largely influences the foot contact forces. However in case of contact redundancy, where not all the contact forces are dominated by the weight of the robot, it could be reasonable to first optimize all the contact forces according to environment rigidity and balance condition, and then compute the CoM target position that is compatible with the desired contact forces.

V. CONCLUSIONS AND FUTURE WORKS

In this paper, a reactive control approach is proposed for balancing on multiple non-rigid contacts during whole-body task execution. The contribution here is to endow existing whole-body controllers, which usually work for non-rigid environments, with the ability to adapt to unknown non-rigid environments. The goal of this adaptation is to obtain sufficient reaction forces from the environment to support the whole-body motion in a relatively natural way.

The proposed approach finds optimal robot control inputs (τ) and optimal contact forces by solving an optimization

problem, which takes into account all the elementary motion task objectives, local support contact states, as well as various constraints. The solution satisfies whole-body dynamics constraint and friction cone constraints to ensure whole-body balance. Experiments on a simulated iCub robot are conducted to demonstrate that this approach allows the humanoid robot to maintain balance in non-rigid environments.

One future research direction is to further study how to combine the proposed approach, which is reactive and adapts to non-rigid environments, with some motion planning techniques, which may optimize the robot motions from a global point of view, but are usually not adaptable to unknown non-rigid environments.

Moreover, the current version of this reactive whole-body controller handles contacts for balance support. It would be interesting to extend such whole-body control by incorporating other types of elementary physical interaction tasks, such as interactions with humans through end-effector contacts. One way to achieve this goal is to apply an impedance controller, which has been applied to robotic manipulators to achieve safe and robust interactions [16,21], to locally control the interaction with humans.

References

[1] O. Khatib, L. Sentis, and J.-H. Park, "A unified framework for whole-body humanoid robot control with multiple constraints and contacts," in *European Robotics Symposium 2008*, ser. Springer Tracts in Advanced Robotics. Springer Berlin / Heidelberg, 2008, vol. 44, pp. 303–312.

[2] L. Sentis, J. Park, and O. Khatib, "Compliant control of multi-contact and center of mass behaviors in humanoid robots," *IEEE Transactions on Robotics*, vol. 26, no. 3, pp. 483–501, june 2010.

[3] L. Righetti, J. Buchli, M. Mistry, M. Kalakrishnan, and S. Schaal, "Optimal distribution of contact forces with inverse dynamics control," *The International Journal of Robotics Research*, 2013.

[4] Y. Abe, M. da Silva, and J. Popović, "Multiobjective control with frictional contacts," in *Proceedings of the ACM SIGGRAPH/Eurographics symposium on Computer animation*, 2007, pp. 249–258.

[5] M. Liu, A. Micaelli, P. Evrard, A. Escande, and C. Andriot, "Interactive dynamics and balance of a virtual character during manipulation tasks," in *IEEE International Conference on Robotics and Automation*, may 2011, pp. 1676–1682.

[6] J. Salini, S. Barthlemy, P. Bidaud, and V. Padois, "Whole-body motion synthesis with lqp-based controller - application to icub," in *Cognitive Systems Monographs : Modeling, Simulation and Optimization of Bipedal Walking*, K. Mombaur and K. Berns, Eds. Springer Berlin Heidelberg, 2013, vol. 18, pp. 119–210.

[7] L. Saab, O. Ramos, F. Keith, N. Mansard, P. Soueres, and J.-Y. Fourquet, "Dynamic whole-body motion generation under rigid contacts and other unilateral constraints," *Robotics, IEEE Transactions on*, vol. 29, no. 2, pp. 346–362, 2013.

[8] B. Stephens and C. Atkeson, "Dynamic balance force control for compliant humanoid robots," in *IEEE/RSJ International Conference on Intelligent Robots and Systems*, oct. 2010, pp. 1248–1255.

[9] F. Nori, S. Traversaro, J. Eljaik, F. Romano, A. Del Prete, and D. Pucci, "icub whole-body control through force regulation on rigid noncoplanar contacts," *Frontiers in Robotics and AI*, 2015.

[10] U. Muico, Y. Lee, J. Popović, and Z. Popović, "Contact-aware nonlinear control of dynamic characters," *ACM Trans. Graph.*, vol. 28, pp. 81:1–81:9, July 2009.

[11] O. Khatib, "A unified approach for motion and force control of robot manipulators: The operational space formulation," *Robotics and Automation, IEEE Journal of*, vol. 3, no. 1, pp. 43–53, 1987.

[12] N. Hogan, "Impedance control: An approach to manipulation - part i: Theory; part ii: Implementation; part iii: Applications," *Journal of dynamic systems, measurement, and control*, vol. 107, no. 1, pp. 1–24, 1985.

[13] L. Love and W. Book, "Environment estimation for enhanced impedance control," in *IEEE International Conference on Robotics and Automation*, vol. 2, May 1995, pp. 1854–1859 vol.2.

[14] T. Tsumugiwa, R. Yokogawa, and K. Hara, "Variable impedance control based on estimation of human arm stiffness for human-robot cooperative calligraphic task," in *IEEE International Conference on Robotics and Automation*, vol. 1, 2002, pp. 644–650 vol.1.

[15] J. Buchli, E. Theodorou, F. Stulp, and S. Schaal, "Variable impedance control-a reinforcement learning approach." in *Robotics: Science and Systems*, 2010.

[16] C. Yang, G. Ganesh, S. Haddadin, S. Parusel, A. Albu-Schaeffer, and E. Burdet, "Human-like adaptation of force and impedance in stable and unstable interactions," *IEEE Transactions on Robotics*, vol. 27, no. 5, pp. 918–930, Oct 2011.

[17] K. Bouyarmane and A. Kheddar, "Fem-based static posture planning for a humanoid robot on deformable contact support," in *11th IEEE-RAS International Conference on Humanoid Robots*, Oct 2011, pp. 487–492.

[18] T. Bretl and S. Lall, "Testing static equilibrium for legged robots," *IEEE Transactions on Robotics*, vol. 24, no. 4, pp. 794–807, aug. 2008.

[19] P.-B. Wieber, "Trajectory free linear model predictive control for stable walking in the presence of strong perturbations," in *Humanoid Robots, 2006 6th IEEE-RAS International Conference on*, Dec 2006, pp. 137–142.

[20] X. Merlhiot, J. Le Garrec, G. Saupin, and A. G., "The xde mechanical kernel: Efficient and robust simulation of multibody dynamics with intermittent nonsmooth contacts," in *The Second Joint International Conference on Multibody System Dynamics*, 2012.

[21] A. Albu-Schäffer, C. Ott, and G. Hirzinger, "A unified passivity-based control framework for position, torque and impedance control of flexible joint robots," *The International Journal of Robotics Research*, vol. 26, no. 1, pp. 23–39, 2007.

4 Balancing on compliant contacts: model-based control approach

When a model of the environment is available or has been incrementally learnt, using this model does not only provide the necessary adaptation to the new conditions but allows to obtain efficient behaviours that could not be obtained otherwise. It thus makes much sense to try to model the compliant environment.

4.1 Model modifications induced by compliant contacts

When dealing with compliant contacts, modifications are induced in the equation of motion and kinematic constraints expression. The former writes

$$M(q)\dot{\nu} + C(q,\nu)\nu + G(q) = B\tau + J_{rigid}^{\top}(q)f_{rigid} + J_{comp}^{\top}(q)f_{comp}, \tag{5}$$

while the latter is decomposed in two sub-equations

$$J_{rigid}(q)\dot{\nu} + \dot{J}_{rigid}(q)\nu = 0 \tag{6a}$$

$$J_{comp}(q)\dot{\nu} + \dot{J}_{comp}(q)\nu = \ddot{p}_{\mathcal{C}_{comp}}, \tag{6b}$$

where $J_{rigid}^{\top}(q)$, f_{rigid}, $J_{comp}^{\top}(q)$ and f_{comp} respectively represent the contact Jacobian in the rigid contact directions, the associated rigid contact wrench, the contact Jacobian in the compliant contact directions and the associated compliant contact wrench. Without loss of generality, contacts are here supposed to be either strictly rigid or compliant[2]. $\ddot{p}_{\mathcal{C}_{comp}}$ is the compliant contact points linear and angular acceleration which is assumed to be a function of the state of the contact points and of the derivative of the compliant contact wrench[3] $\ddot{p}_{\mathcal{C}_{comp}} = z\left(p_{\mathcal{C}_{comp}}, R_{\mathcal{C}_{comp}}, \dot{p}_{\mathcal{C}_{comp}}, \omega_{\mathcal{C}_{comp}}, f_{comp}\right)$.

4.2 Augmentation of the relative degree of the controlled outputs

From the modified model, it can be shown that f cannot be considered as an independent intermediate control input any longer as its evolution is subject to the contact points dynamics which is a function of $\dot{f}$. $\dot{f}$ becomes the new independent intermediate control input and it can be concluded that compliant contacts augment the relative degree of the controlled outputs. This means that Equation (4) has to be differentiated in order to relate $\dot{f}$ to the desired center of mass behaviour. The computed contact force derivative can then be fed into Equation (6b). Assuming that a good measurement of the compliant contact forces is available and that z can be estimated with high bandwidth and precision through measurement, whole-body dynamics estimation and/or contact model parameters estimation, one can then directly solve the whole-body control problem.

---

[2]A given contact point can actually be rigid in some direction while compliant in other orthogonal ones.

[3]As an intuition, consider the example of a mono-dimensional spring-damper system described by the scalar relation $f = K(x - x_0) + b\dot{x}$, the contact point acceleration can be written $\ddot{x} = \frac{1}{b}(\dot{f} - K\dot{x})$.

Even if not formulated in this way, this is the approach retained in [31] where a "practical" implementation is proposed. The proposed controller regulates both linear momentum and angular momentum about the center of mass of the robot by controlling the contact forces at soft contact surfaces[4]. Assuming that contact forces at the compliant surfaces are known (i.e. via force-torque sensors) at the current instant, desired contact forces at the rigid contacts are calculated in order to provide the required rate of change of the robot's momentum. However, since compliant contact forces are functions of surface deformations, there is not any control on them at the current instant. Nonetheless, it is possible to control those forces in the next instant by controlling the acceleration of the contact points. This can be done by predicting one step ahead in time the compliant contact forces given the currently measured ones and the contact model z. To implement the proposed method in practice, stiffness and damping coefficients of the contact model have to be estimated beforehand by using contact model parameter estimation methods such as in [32], [33], [34]. Details of the proposed implementation can be found in the paper hereafter included.

---

[4]rigid contact can be accounted for as well without modifying the proposed method itself and with the advantage of easing the estimation of the state of the floating base

Balance Control Strategy for Legged Robots with Compliant Contacts

Morteza Azad and Michael N Mistry

Abstract— This paper proposes a momentum-based balancing controller for robots which have non-rigid contacts with their environments. This controller regulates both linear momentum and angular momentum about the center of mass of the robot by controlling the contact forces. Compliant contact models are used to determine the contact forces at the contact points. Simulation results show the performance of the controller on a four-link planar robot standing on various compliant surfaces while unknown external forces in different directions are acting on the center of mass of the robot.

I. Introduction

Balancing for legged robots, which is in fact preventing them from falling over, has always the highest priority in controlling their motions. This problem becomes much more challenging if the supporting surface (i.e. usually the ground) is not "*rigid*". In reality, there is no completely rigid surface but in practice we can assume a surface to be rigid if it is stiff enough (i.e. deflection is negligible). Many of existing legged robots are able to keep their balance on rigid surfaces but still most of them have difficulties in dealing with compliant supporting surfaces. To balance a legged robot on a soft surface (e. g. on a thick carpet), the compliance of the contact has to be considered by the controller, otherwise the robot fails to balance and falls over.

Compliant contacts between robots and their environments have been studied by some researchers in the area of humanoids [5], grasping [16], animated characters [12], etc. However, there have not been much efforts on balancing legged robots on compliant surfaces. In this paper, we tackle this problem and introduce a momentum-based balancing controller which takes into account the effects of non-rigid contacts between the robot and its environment. A momentum-based controller, controls both linear momentum and angular momentum about the center of mass (CoM) of the robot. This type of controller is first suggested by Goswami and Kallem [9] and then extensively used in recent years by other researchers [1], [3], [10], [13], [14].

In this paper, we present a method to implement a momentum-based control strategy to balance legged robots on compliant surfaces. This is done by controlling the supporting forces at the contact points. Non-linear compliant contact models are used to calculate both normal and friction forces between the robot and its environment. The normal force model is the one that is introduced in [4]. It is a modified version of the well-known Hunt-Crossley model [11], [15] and is shown to be more accurate. We also use the

Morteza Azad and Michael N. Mistry are with the School of Computer Science, University of Birmingham, Edgbaston, UK. m.azad and m.n.mistry at bham.ac.uk

friction force model in [2] which has a similar non-linearity to the normal force model. To implement the proposed method in practice, stiffness and damping coefficients of the contact model have to be estimated beforehand by using contact model parameter estimation methods such as [6], [7], [8]. Note that, using other contact models (e. g. linear models) does not influence the proposed control strategy. So, in practice, any valid contact model which experimentally fits the contact between the robot and its environment can be incorporated in this control algorithm.

Our proposed strategy converts the balance problem to a linear constrained optimization problem which its output is the vector of desired joint accelerations. It first calculates the desired supporting forces at the contact points by using the robot's momentum. Then, based on the contact model and by using the Jacobian of the contact points, it converts the desired contact forces to the desired joint accelerations. At the end, by using the inverse dynamics of the robot, the joint torques are calculated.

Finally, we implement the proposed control strategy on a planar four-link robot in simulation. The robot is to keep its balance while it is being disturbed by unknown external forces applying to its CoM in vertical and horizontal directions.

II. Compliant Contact Model

This section briefly explains the contact model which is used to calculate normal and tangential contact forces in our dynamics simulator.

A. The Geometry of the Contact

We model each contact surface as a set of contact points. Therefore, the resultant contact force is the sum of the contact forces at the contact points and the location of the center of pressure depends on this summation and it may be none of these contact points. The compliant (normal and tangential) contact forces at each contact point depend on relative (normal and shear) deformations and their rates of changes at that point. In general, the normal (to the surface) at each contact point is not necessarily in the vertical direction. So, we define a local coordinate frame at each contact point which its z axis is in the direction of the normal vector. These coordinate frames are fixed with respect to the inertial frame. Therefore, displacements of each contact point in its local frame are equal to the deformations at that point.

Let $\mathbf{R}_i$ represent the rotation matrix of the ith local coordinate frame with respect to the inertial frame XYZ. Also let $\mathbf{p}_i = (x_i, y_i, z_i)^T$ and $\dot{\mathbf{p}}_i = (\dot{x}_i, \dot{y}_i, \dot{z}_i)^T$ represent the position and velocity of the ith contact point (cp_i) in the

inertial frame and $\mathbf{r}_i = (x_{r_i}, y_{r_i}, z_{r_i})^T$ represent the origin of the ith local frame with respect to the inertial frame ($\dot{\mathbf{r}}_i = 0$). Therefore, the relative position and velocity of cp_i in its local frame is

$$\boldsymbol{\eta}_i = \mathbf{R}_i^T(\mathbf{p}_i - \mathbf{r}_i) = \mathbf{R}_i^T \begin{bmatrix} x_i \\ y_i \\ z_i \end{bmatrix} - \mathbf{R}_i^T \begin{bmatrix} x_{r_i} \\ y_{r_i} \\ z_{r_i} \end{bmatrix} = \begin{bmatrix} \xi_i \\ \epsilon_i \\ \zeta_i \end{bmatrix} \quad (1)$$

and

$$\dot{\boldsymbol{\eta}}_i = \mathbf{R}_i^T \dot{\mathbf{p}}_i = \begin{bmatrix} \dot{\xi}_i \\ \dot{\epsilon}_i \\ \dot{\zeta}_i \end{bmatrix}, \quad (2)$$

where $\mathbf{R}_i^T$ is the transpose of $\mathbf{R}_i$ and $\dot{\mathbf{R}}_i = 0$. Note that at the instant of the beginning of the contact $\mathbf{p}_i = \mathbf{r}_i$.

B. Normal Force Model

To calculate the contact normal force we use the contact model in [4] which is

$$f_n = \max(0, k\delta^{\frac{3}{2}} + \lambda\delta^{\frac{1}{2}}\dot{\delta}), \quad (3)$$

where f_n is the normal force, k and λ are the stiffness and damping coefficients and δ is the local normal deformation at the contact point. According to (1), the local deformation in the normal direction at cp_i is $\delta_i = -\zeta_i$. So, we can write the normal force model for this point as

$$f_{n_i} = \begin{cases} 0 & \text{if } \zeta_i > 0 \\ \max(0, -\sqrt{-\zeta_i}(k_i\zeta_i + \lambda_i\dot{\zeta}_i)) & \text{if } \zeta_i \leq 0 \end{cases} \quad (4)$$

where k_i and λ_i are the coefficients of stiffness and damping at cp_i, respectively. Note that f_{n_i} is always positive implying that the normal force is unilateral.

C. Tangential Force Model

Tangential or friction force is calculated by using the model which is introduced in [2]. According to this model, when there is no slipping, the tangential force at cp_i is

$$\mathbf{f}_{\mathbf{s}i} = -\sqrt{-\zeta_i}(k_i\mathbf{u}_i + \lambda_i\dot{\mathbf{u}}_i), \quad (5)$$

where $\mathbf{f}_{\mathbf{s}i}$ is a 2×1 vector, $\mathbf{u}_i$ is the shear deformation at cp_i and $\dot{\mathbf{u}}_i$ is the rate of change of $\mathbf{u}_i$ which are

$$\mathbf{u}_i = \begin{bmatrix} \xi_i \\ \epsilon_i \end{bmatrix} \quad \text{and} \quad \dot{\mathbf{u}}_i = \begin{bmatrix} \dot{\xi}_i \\ \dot{\epsilon}_i \end{bmatrix}. \quad (6)$$

In the case of slipping, friction force is limited to the friction cone and its magnitude is $\mu_i f_{n_i}$, where μ_i is the friction coefficient at cp_i. Note that in this case, (6) is no longer valid and $\dot{\mathbf{u}}$ has to be calculated from

$$\dot{\mathbf{u}} = \frac{\mathbf{f}_{\mathbf{f}i} + \sqrt{-\zeta_i}k_i\mathbf{u}}{-\sqrt{-\zeta_i}\lambda_i}, $$

where $\mathbf{f}_{\mathbf{f}i}$ is the friction force at cp_i as

$$\mathbf{f}_{\mathbf{f}i} = \begin{cases} \mathbf{f}_{\mathbf{s}i} & \text{if } |\mathbf{f}_{\mathbf{s}i}| < \mu_i f_{n_i} \\ \frac{\mu_i f_{n_i}}{|\mathbf{f}_{\mathbf{s}i}|}\mathbf{f}_{\mathbf{s}i} & \text{otherwise} \end{cases} \quad (7)$$

For more details on the contact model readers are encouraged to refer to [2].

III. CONTROL STRATEGY

In this section, we introduce a balancing control algorithm for a robot with compliant contacts with the environment. The main difference between rigid and compliant contacts is that, in the latter case, the contact points have non-zero accelerations. Controlling these accelerations allows us to control the external forces acting on the robot and consequently to control the robot's momentum.

The strategy of the proposed controller is to determine desired values for the contact point accelerations (and consequently for the joint accelerations) to achieve the desired rate of change of the robot's momentum which is denoted by $\dot{\mathbf{h}}_d$ in this paper. We calculate $\dot{\mathbf{h}}_d$ by using a momentum-based control algorithm which controls both linear and angular momenta of the robot. The control laws for this controller are

$$\dot{\mathbf{h}}_d = \begin{bmatrix} mk_p(\mathbf{c}_d - \mathbf{c}) + mk_v(\dot{\mathbf{c}}_d - \dot{\mathbf{c}}) \\ k_l(\mathbf{l}_d - \mathbf{l}) \end{bmatrix}, \quad (8)$$

where m is the total mass of the robot, $\mathbf{l}$ is the angular momentum about the CoM, $\mathbf{c}$ is the location of the CoM and k_p, k_v and k_l are the gains of the controller. Also subscript $_d$ represents the desired value of each variable.

A. Contact Model for the Controller

For the purpose of the controller's calculations we use the same contact model that already described in section II but we limit the contact point accelerations by the controller to ensure that there is no slipping nor breaking of the contacts.

1) Constraints: According to (4), the necessary condition for the normal force to prevent breaking of the contact at cp_i is

$$k_i\zeta_i + \lambda_i\dot{\zeta}_i < 0, \quad (9)$$

which, by using (1), it can be written as

$$\mathbf{S}_\zeta \mathbf{R}_i^T(k_i(\mathbf{p}_i - \mathbf{r}_i) + \lambda_i\dot{\mathbf{p}}_i) < 0, \quad (10)$$

where $\mathbf{S}_\zeta = [0\ 0\ 1]$.

To avoid slipping, the friction force is limited by the controller to be inside the friction cone. Here, to have linear constraints, we approximate the friction cone by a convex tetrahedral cone. By using this approximation we have

$$|-\delta_i^{\frac{1}{2}}(k_i\xi_i + \lambda_i\dot{\xi}_i)| < -\mu_i\frac{\sqrt{2}}{2}\delta_i^{\frac{1}{2}}(k_i\zeta_i + \lambda_i\dot{\zeta}_i), \quad (11)$$

and

$$|-\delta_i^{\frac{1}{2}}(k_i\epsilon_i + \lambda_i\dot{\epsilon}_i)| < -\mu_i\frac{\sqrt{2}}{2}\delta_i^{\frac{1}{2}}(k_i\zeta_i + \lambda_i\dot{\zeta}_i), \quad (12)$$

which any of them can be written as two inequality constraints and therefore, in matrix forms as

$$\mathbf{S}_\xi \mathbf{R}_i^T(k_i(\mathbf{p}_i - \mathbf{r}_i) + \lambda_i\dot{\mathbf{p}}_i) < \mathbf{0}, \quad (13)$$

and

$$\mathbf{S}_\epsilon \mathbf{R}_i^T(k_i(\mathbf{p}_i - \mathbf{r}_i) + \lambda_i\dot{\mathbf{p}}_i) < \mathbf{0}, \quad (14)$$

where

$$\mathbf{S}_\xi = \begin{bmatrix} -1 & 0 & \frac{\sqrt{2}}{2}\mu_i \\ 1 & 0 & \frac{\sqrt{2}}{2}\mu_i \end{bmatrix} \quad \text{and} \quad \mathbf{S}_\epsilon = \begin{bmatrix} 0 & -1 & \frac{\sqrt{2}}{2}\mu_i \\ 0 & 1 & \frac{\sqrt{2}}{2}\mu_i \end{bmatrix}.$$

So we can write all five constraints (10), (13) and (14) for cp_i as

$$\mathbf{A}_i(\mathbf{p}_i - \mathbf{r}_i) + \mathbf{B}_i\dot{\mathbf{p}}_i < \mathbf{0}, \tag{15}$$

where $\mathbf{A}_i = k_i\mathbf{S}\mathbf{R}_i^T$, $\mathbf{B}_i = \lambda_i\mathbf{S}\mathbf{R}_i^T = (\lambda_i/k_i)\mathbf{A}_i$ and $\mathbf{S} = [\mathbf{S}_\xi^T \ \mathbf{S}_\epsilon^T \ \mathbf{S}_\zeta^T]^T$. Therefore, constraint (15) for all contact points will be

$$\mathbf{A}(\mathbf{p} - \mathbf{r}) + \mathbf{B}\dot{\mathbf{p}} < \mathbf{0}, \tag{16}$$

where $\mathbf{p} = [\mathbf{p}_1^T \ \mathbf{p}_2^T \ \ldots \ \mathbf{p}_n^T]^T$, $\mathbf{r} = [\mathbf{r}_1^T \ \mathbf{r}_2^T \ \ldots \ \mathbf{r}_n^T]^T$, n is the total number of the contact points and

$$\mathbf{A} = \begin{bmatrix} \mathbf{A}_1 & \mathbf{0}_{5\times3} & \ldots & \mathbf{0}_{5\times3} \\ \mathbf{0}_{5\times3} & \mathbf{A}_2 & \ldots & \mathbf{0}_{5\times3} \\ \vdots & \vdots & \ddots & \vdots \\ \mathbf{0}_{5\times3} & \mathbf{0}_{5\times3} & \ldots & \mathbf{A}_n \end{bmatrix}, \mathbf{B} = \begin{bmatrix} \mathbf{B}_1 & \mathbf{0}_{5\times3} & \ldots & \mathbf{0}_{5\times3} \\ \mathbf{0}_{5\times3} & \mathbf{B}_2 & \ldots & \mathbf{0}_{5\times3} \\ \vdots & \vdots & \ddots & \vdots \\ \mathbf{0}_{5\times3} & \mathbf{0}_{5\times3} & \ldots & \mathbf{B}_n \end{bmatrix}.$$

2) External Forces: Assuming that there is no loss of contact and slipping at the contact points, the contact force at cp_i in its local frame is

$$\begin{aligned} \mathbf{f}_i &= -\delta_i^{\frac{1}{2}} k_i \boldsymbol{\eta}_i - \delta_i^{\frac{1}{2}} \lambda_i \dot{\boldsymbol{\eta}}_i \\ &= -\delta_i^{\frac{1}{2}} (k_i \mathbf{R}_i^T(\mathbf{p}_i - \mathbf{r}_i) + \lambda_i \mathbf{R}_i^T \dot{\mathbf{p}}_i). \end{aligned} \tag{17}$$

Transforming $\mathbf{f}_i$ to the inertial frame yields

$$\mathbf{R}_i\mathbf{f}_i = -\delta_i^{\frac{1}{2}} (k_i(\mathbf{p}_i - \mathbf{r}_i) + \lambda_i \dot{\mathbf{p}}_i). \tag{18}$$

where $\mathbf{R}_i\mathbf{f}_i$ is a 3×1 vector representing the contact forces at cp_i expressed in the inertial frame.

3) External Moments: For the controller's calculations we also need the moment of the external forces about the CoM. Let $\mathbf{d}_i = \mathbf{p}_i - \mathbf{c}$ denote the relative position of cp_i to the CoM in the inertial frame. By defining a 3×3 skew symmetric matrix $\mathbf{D}_i$ as

$$\mathbf{D}_i = \begin{bmatrix} 0 & -d_{z_i} & d_{y_i} \\ d_{z_i} & 0 & -d_{x_i} \\ -d_{y_i} & d_{x_i} & 0 \end{bmatrix},$$

where d_{x_i}, d_{y_i} and d_{z_i} are the components of $\mathbf{d}_i$ in x, y and z directions, respectively, we can write the external moment for the ith contact force about the CoM as

$$\boldsymbol{\tau}_i = \mathbf{D}_i\mathbf{R}\mathbf{f}_i. \tag{19}$$

4) The Rate of Change of Momentum: The rate of change of the robot's momentum about its CoM due to the contact forces at cp_i in spatial form is

$$\begin{aligned} \dot{\mathbf{h}}_i &= -\delta_i^{\frac{1}{2}} \begin{bmatrix} k_i\mathbf{D}_i(\mathbf{p}_i - \mathbf{r}_i) + \lambda_i\mathbf{D}_i\dot{\mathbf{p}}_i \\ k_i(\mathbf{p}_i - \mathbf{r}_i) + \lambda_i\dot{\mathbf{p}}_i \end{bmatrix} \\ &= \mathbf{M}_i(\mathbf{p}_i - \mathbf{r}_i) + \mathbf{N}_i\dot{\mathbf{p}}_i, \end{aligned} \tag{20}$$

where

$$\mathbf{M}_i = -k_i\delta_i^{\frac{1}{2}} \begin{bmatrix} \mathbf{D}_i \\ I_{3\times3} \end{bmatrix}, \mathbf{N}_i = -\lambda_i\delta_i^{\frac{1}{2}} \begin{bmatrix} \mathbf{D}_i \\ I_{3\times3} \end{bmatrix} = \frac{\lambda_i}{k_i}\mathbf{M}_i, \tag{21}$$

and $I_{3\times3}$ is a 3×3 identity matrix. Thus, the total rate of change of the robot's momentum is

$$\dot{\mathbf{h}} = \sum_{i=1}^n \dot{\mathbf{h}}_i + \mathbf{G} = \mathbf{M}(\mathbf{p} - \mathbf{r}) + \mathbf{N}\dot{\mathbf{p}} + \mathbf{G}, \tag{22}$$

where $\mathbf{M} = [\mathbf{M}_1 \ \mathbf{M}_2 \ \ldots \ \mathbf{M}_n]$, $\mathbf{N} = [\mathbf{N}_1 \ \mathbf{N}_2 \ \ldots \ \mathbf{N}_n]$ and $\mathbf{G}$ is the external moment of the gravity about the CoM.

B. Desired Accelerations

Due to the compliance of the contact, the external forces acting on the robot and therefore $\dot{\mathbf{h}}$ are known in the current instant of simulation and cannot be changed by the control torques. However, these torques are able to control the value of $\dot{\mathbf{h}}$ in the next instant of simulation. Hence, the objective of the controller is to control the external forces in the next instant by determining the desired values of the joint accelerations and torques in the current instant of simulation.

To calculate the desired external forces in the next instant of simulation, we need to predict the state variables ($\mathbf{q}$ and $\dot{\mathbf{q}}$) in that instant. Assuming that the time interval between two successive instants of simulation is Δt and by using first-order linear integration method we have

$$\mathbf{p}_{\Delta t} = \mathbf{p} + \Delta t\,\dot{\mathbf{p}} \quad \text{and} \quad \dot{\mathbf{p}}_{\Delta t} = \dot{\mathbf{p}} + \Delta t\,\ddot{\mathbf{p}}, \tag{23}$$

where $\mathbf{p}_{\Delta t}$ and $\dot{\mathbf{p}}_{\Delta t}$ are the controller's predictions of $\mathbf{p}$ and $\dot{\mathbf{p}}$ for the next instant of simulation, respectively, and $\ddot{\mathbf{p}}$ is the contact point acceleration. Also let $\mathbf{M}_{\Delta t}$ and $\mathbf{N}_{\Delta t}$ represent the values of $\mathbf{M}$ and $\mathbf{N}$ in the next instant, respectively. These values can be calculated by replacing (23) into (21) and also replacing $\mathbf{c}$ with $\mathbf{c}_{\Delta t} = \mathbf{c} + \Delta t\,\dot{\mathbf{c}}$ for calculating $\mathbf{d}_i$.

Therefore, the rate of change of the robot's momentum in the next instant is

$$\dot{\mathbf{h}}_{\Delta t} = \mathbf{M}_{\Delta t}(\mathbf{p}_{\Delta t} - \mathbf{r}) + \mathbf{N}_{\Delta t}\dot{\mathbf{p}}_{\Delta t} \tag{24}$$

Substituting (23) into (24) yields

$$\dot{\mathbf{h}}_{\Delta t} = \mathbf{M}_{\Delta t}(\mathbf{p} - \mathbf{r}) + (\mathbf{M}_{\Delta t}\,\Delta t + \mathbf{N}_{\Delta t})\dot{\mathbf{p}} + \mathbf{N}_{\Delta t}\,\Delta t\,\ddot{\mathbf{p}}, \tag{25}$$

which is a linear relationship between the rate of change of momentum ($\dot{\mathbf{h}}$) and the contact point accelerations ($\ddot{\mathbf{p}}$). Note that $\mathbf{M}$ and $\mathbf{N}$ are functions of the joint angles and therefore $\mathbf{M}_{\Delta t}$ and $\mathbf{N}_{\Delta t}$ are functions of the joint angles and joint velocities.

From the kinematics of the robot we can write

$$\dot{\mathbf{p}} = \mathbf{J}\dot{\mathbf{q}} \implies \ddot{\mathbf{p}} = \dot{\mathbf{J}}\dot{\mathbf{q}} + \mathbf{J}\ddot{\mathbf{q}}, \tag{26}$$

where $\mathbf{J}$ is the Jacobian of the contact points with respect to the inertial frame. Replacing (26) into (25) yields

$$\dot{\mathbf{h}}_{\Delta t} = \boldsymbol{\alpha}\ddot{\mathbf{q}} + \boldsymbol{\beta}, \tag{27}$$

where

$$\boldsymbol{\alpha} = \mathbf{N}_{\Delta t}\,\Delta t\,\mathbf{J} \tag{28}$$

$$\begin{aligned} \boldsymbol{\beta} &= \mathbf{M}_{\Delta t}(\mathbf{p} - \mathbf{r}) + \mathbf{G} \\ &+ ((\mathbf{M}_{\Delta t}\,\Delta t + \mathbf{N}_{\Delta t})\mathbf{J} + \mathbf{N}_{\Delta t}\,\Delta t\,\dot{\mathbf{J}})\dot{\mathbf{q}} \end{aligned} \tag{29}$$

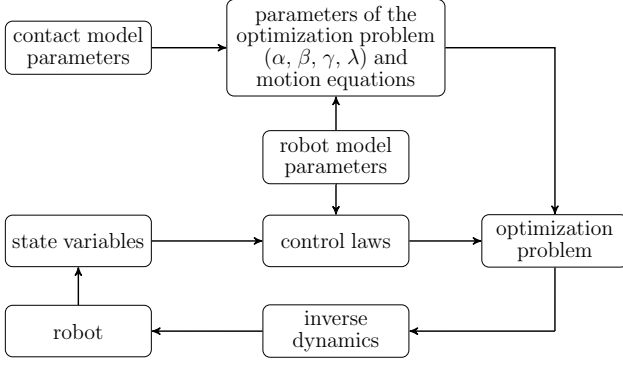which is a linear relationship between the rate of change of

Fig. 1. graphical demonstration of the control algorithm

momentum ($\dot{\mathbf{h}}$) and the joint accelerations ($\ddot{\mathbf{q}}$).

Also by replacing (23) into (16), the constraints will be

$$\mathbf{A}(\mathbf{p} - \mathbf{r}) + (\mathbf{A}\Delta t + \mathbf{B})\dot{\mathbf{p}} + \mathbf{B}\Delta t\ddot{\mathbf{p}} < \mathbf{0}, \qquad (30)$$

which by using (26), they can be written as

$$\boldsymbol{\gamma}\ddot{\mathbf{q}} + \boldsymbol{\phi} < 0, \qquad (31)$$

where

$$\boldsymbol{\gamma} = \mathbf{B}\Delta t\mathbf{J} \qquad (32)$$

$$\boldsymbol{\phi} = \mathbf{A}(\mathbf{p} - \mathbf{r}) + ((\mathbf{A}\Delta t + \mathbf{B})\mathbf{J} + \mathbf{B}\Delta t\dot{\mathbf{J}})\dot{\mathbf{q}}. \qquad (33)$$

Therefore, the balancing control problem becomes a constrained linear optimization problem with the objective function of

$$\ddot{\mathbf{q}}_d = ArgMin(||\boldsymbol{\alpha}\ddot{\mathbf{q}} + \boldsymbol{\beta} - \dot{\mathbf{h}}_d||) \qquad (34)$$

subject to the constraints in (31) and also the motion equations of the base frame (i.e. the floating base) which are due to the under-actuation. Finally, by using inverse dynamics methods, we can calculate the desired joint torques according to the desired joint accelerations.

The control algorithm is graphically shown in Fig. 1. Contact model parameters (k_i, λ_i and μ_i), inertial parameters of the robot and state variables ($\mathbf{q}$ and $\dot{\mathbf{q}}$) are used to calculate the parameters of the objective function ($\boldsymbol{\alpha}$ and $\boldsymbol{\beta}$) and the constraints ($\boldsymbol{\gamma}$ and $\boldsymbol{\phi}$) and motion equations of the floating base. Control laws in (8) are calculated by using the robot model and the state variables. Output of the optimization problem is a vector of the desired joint accelerations ($\ddot{\mathbf{q}}_d$) which goes through the inverse dynamic function and gives us the required joint torques for applying to the robot.

IV. EXAMPLE: A PLANAR FOUR-LINK ROBOT

In this section, we implement our proposed control algorithm on a four-link planar robot in simulation. The controller is to balance the robot on the compliant ground while external disturbances are applying to the robot. The robot consists of a foot, a shank, a thigh and a torso. A schematic diagram of the robot is shown in Fig. 2. The foot has three degrees of freedom (DoF) which are under-actuated and denoted by q_1, q_2 and q_3. In fact, q_1 and q_2 are the displacements of the origin of the foot in horizontal and
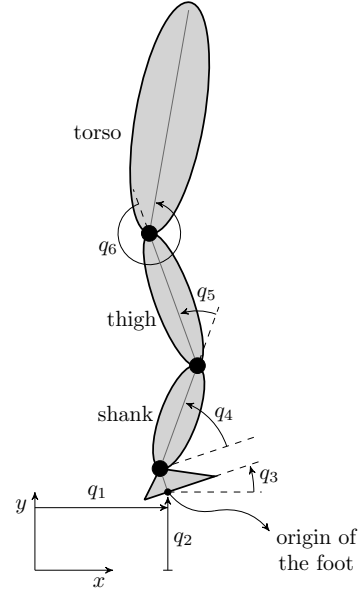

Fig. 2. Schematic diagram of the robot model and its coordinates

TABLE I
INERTIAL PARAMETERS OF THE PLANAR ROBOT (SI UNITS).

link	mass	length	I_G	l_c
foot	1.86	0.085	0.0038	0.051
shank	6.4	0.408	0.0504	0.257
thigh	20.26	0.425	0.1052	0.268
torso	40.6	0.68	1.28	0.422

vertical directions, respectively, and q_3 is the rotation angle of the foot. Thus, the whole robot has six DoF which only three of them (i.e. q_4, q_5 and q_6) are actuated. The lengths of the links and their inertial parameters are mentioned in Table I. In this table, I_G is the moment of inertia about the CoM of each link and l_c is the location of the CoM of each link with respect to its predecessor joint. For the foot, the length is the distance between the origin of the foot and the ankle joint.

The width of the foot (in x direction) is assumed to be 25cm. We assume that the heel is 5cm behind the origin and the toe is 20cm in front of it. We consider six contact points at the sole of the foot to make contact with the ground. These points are evenly distributed along the sole from the heel to the toe with 5cm distance between every two adjacent points. The desired values of linear and angular momenta in (8) are set to zero. The desired value of the CoM is set to $\mathbf{c}_d = [0.09\ 0.95]^T$ and the controller gains are $k_p = 6$, $k_v = 3$ and $k_l = 3$.

To study the performance of the controller on different contact surfaces, the results of three sets of simulations are presented. The difference is in the parameters of the contact model. For the soft surface we set $k_i = 3 \times 10^4$ and $\lambda_i = 70$, for the medium one we set $k_i = 3 \times 10^5$ and $\lambda_i = 700$ and for the stiff surface we set $k_i = 3 \times 10^6$
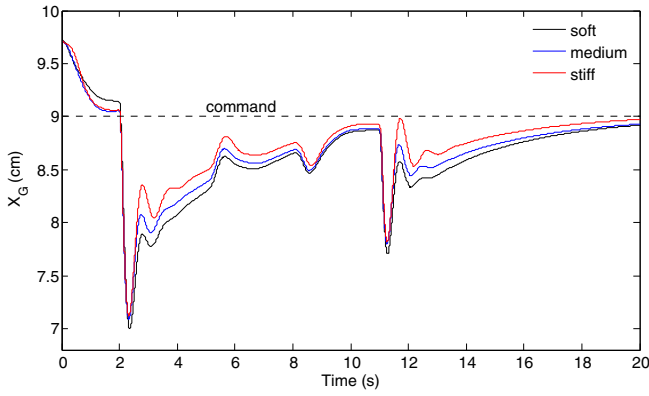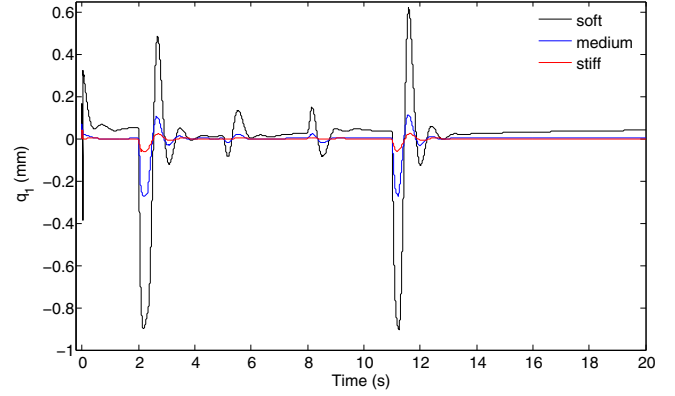
Fig. 3. location of the CoM in x direction

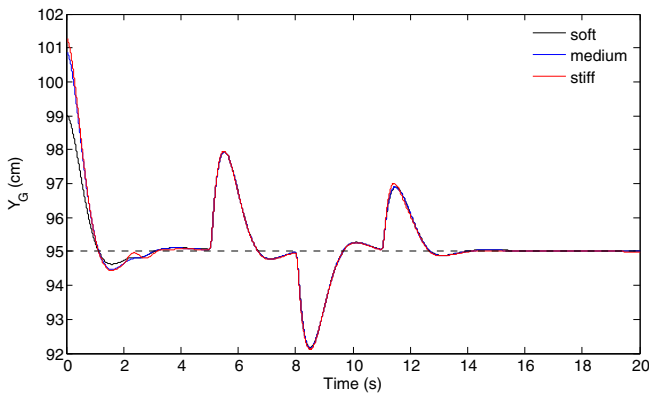Fig. 5. horizontal displacements of the origin of the foot

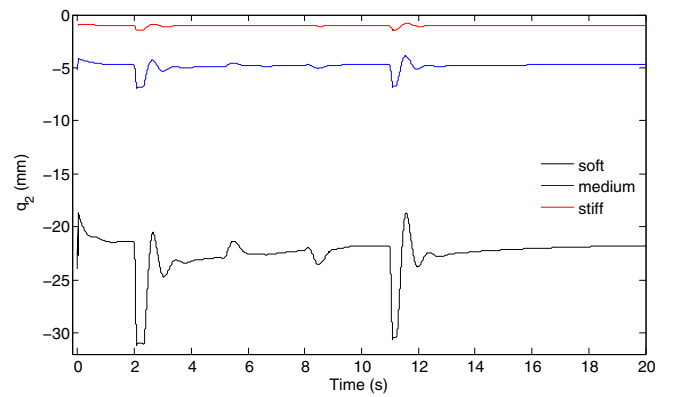Fig. 4. location of the CoM in y direction

Fig. 6. vertical displacements of the origin of the foot

and $\lambda_i = 7 \times 10^3$. These parameters are set to provide different ground deformations under the robot's foot. The initial deformations of the ground due to the weight of the robot for the soft, medium and stiff surfaces are 24mm, 5mm and 1mm, respectively. These are the initial values of q_2. Note that, although k_i and λ_i change linearly for the three different surfaces, the ground deformations change in a non-linear rate which is due to the non-linearity in the contact model. The robot starts from an initial position $q(t = 0) = [0, q_2(t = 0), 0, \frac{\pi}{2} - 0.3, 0.5, -0.4]^T$ with zero joint velocities.

The simulations have been performed by using simulink and Spatial software package [17]. To simulate the dynamics of the robot, we use a continuous variable time step fourth order Runge-Kutta integrator (ode45) with maximum step size of 1ms. However, we run the controller at 1kHz rate and therefore, $\Delta t = 0.001$.

The external disturbances that are applied to the CoM of the robot during 20 seconds of the simulations are: 1) 100N in the $-x$ direction at $t = 2$ for 0.1s, 2) 100N in the y direction at $t = 5$ for 0.1s, 3) 100N in the $-y$ direction at $t = 8$ for 0.1s and 4) 70N in the $-x$ direction and 70N in the y direction at $t = 11$ for 0.1s. Note that the controller does not have any knowledge about these external disturbances.

Figures 3 and 4 show the location of the CoM of the robot in x and y directions, respectively (i.e. x_G and y_G in the plots), for soft, medium and stiff surfaces. Dashed lines show the desired values of the CoM ($\mathbf{c}_d$). As can be seen in these figures, movements of the CoM are almost the same in all three cases which show that the control laws are not affected by the stiffness of the surface. The effects of the external disturbances on the CoM are clear in these figures. At $t = 2$s, the first external disturbance moves the CoM about 2cm in $-x$ direction and has almost no effect on y_G. The second and third disturbances displace the CoM in the vertical direction for about 3cm and the last disturbance moves the CoM in both horizontal and vertical directions. After that, and towards the end of the simulation, the CoM approaches its desired values in x and y directions. Although the rate of convergence is very low in horizontal direction.

Figures 5, 6 and 7 represent the values of q_1, q_2 and q_3, respectively, for all three surfaces. These figures clearly show the differences between the deformations of the surfaces. In the stiff surface, the foot is almost fixed whereas in the medium and soft surfaces it deforms the ground up to about 7mm and 31mm, respectively, at the origin of the foot. The maximum deformation in the soft surface occurs under the heel of the foot and it is 36.4mm. This is shown in
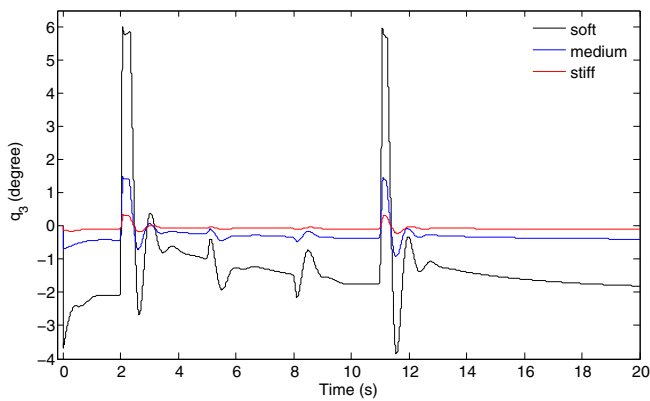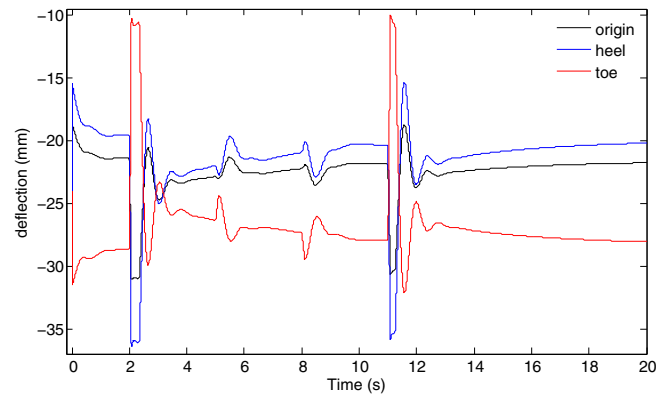
Fig. 7. rotation angle of the foot

Fig. 8. vertical displacements of the foot for the soft surface

Fig. 8 which represents the vertical displacements of the contact points at the origin, heel and toe of the foot for the soft surface. These deformations for our 63kg robot is comparable with deflections of a rubber or cork ground under a human's feet.

As can be seen in Figs. 5, 6 and 7, the foot moves a lot more due to the first and last disturbances rather than the second and third ones. This implies that unknown external forces are much more disturbing in horizontal direction rather than vertical direction. So the foot needs to move more to provide the required supporting forces. Rapid changes at the beginning of the simulations (more clear for soft and medium surfaces) are due to the difference between the initial and desired positions of the foot.

V. CONCLUSION AND FUTURE WORK

In this paper, we proposed a strategy to implement a momentum-based controller on robots with multiple compliant contacts with their environments. The momentum-based controller calculates the desired supporting forces according to the robot's momentum. Our proposed algorithm interprets the desired contact forces as the desired accelerations of the contact points by using the contact model at each contact point. Then, by using the Jacobian of the contact points, which converts the contact point accelerations to the joint accelerations, the balance control problem becomes a linear optimization problem to find the desired joint accelerations. The constraints of this problem ensure that the contacts do not break and no slipping occurs at the contact points.

As an example, we implemented the proposed controller on a planar four-link robot in simulation. It is shown that the controller is able to keep the robot's balance on surfaces with different compliances and in the presence of unknown external disturbances. For the future work we are aiming to implement this controller on a real robot (e.g. an iCub).

VI. ACKNOWLEDGEMENT

REFERENCES

[1] M. Azad, J. Babič and M. Mistry, Effects of hand contact on the stability of a planar humanoid with a momentum based controller, Proc. IEEE-RAS Int. Conf. Humanoid Robots, Madrid, Spain, 18–20 Nov 2014.
[2] M. Azad and R. Featherstone, Modeling the contact between a rolling sphere and a compliant ground plane. Proc. Australasian Conf. Robotics and Automation, Brisbane, Australia, 1–3 Dec 2010.
[3] M. Azad and R. Featherstone, Angular momentum based controller for balancing an inverted double pendulum. RoManSy 19-Robot Design, Dynamics and Control, pp. 251–258, Paris, France, 12–15 June 2012.
[4] M. Azad and R. Featherstone, A new nonlinear model of contact normal force, IEEE Trans. Robotics, 30(3):736–739, June 2014.
[5] K. Bouyarmane and A. Kheddar, FEM-based static posture planning for a humanoid on deformable contact support, IEEE-RAS Int. Conf. Humanoid Robots, pp. 487–492, Bled, Slovenia, 26–28 Oct 2011.
[6] H. Dallali, M. Mosadeghzad, G. A. Medrano-Cerda and N. Docquier, Development of a dynamic simulator for a compliant humanoid robot based on a symbolic multibody approach, IEEE Int. Conf. Mechatronics, pp. 598–603, Vicenza, Italy, Feb 2013.
[7] N. Diolaiti, C. Melchiorri, S. Stramigioli, Contact impedance estimation for robotic systems, IEEE Trans. Robotics, 21(5):925–935, Oct 2005.
[8] D. Erickson, M. Weber, I. Sharf, Contact stiffness and damping estimation for robotic systems, Int. J. Robotics Research, 22(1):41–57, Jan 2003.
[9] A. Goswami and V. Kallem, Rate of change of angular momentum and balance maintenance of biped robots, Proc. IEEE Int. Conf. Robotics and Automation, pp. 3785–3790, New Orleans, LA, April 2004.
[10] A. Hofmann, M. Popovic and H. Herr, Exploiting angular momentum to enhance bipedal center-of-mass control, IEEE Int. Conf. Robotics and Automation, pp.4423–4429, Kobe, Japan, 12–17 May 2009.
[11] K. H. Hunt and F. R. E. Crossley, Coefficient of restitution interpreted as damping in vibroimpact, J. Applied Mechanics, 42(2):440–445, 1975.
[12] S. Jain and C. K. Liu, Controlling physics-based characters using soft contacts, ACM Trans. Graphics, 30(6):163, 2011.
[13] S. H. Lee and A. Goswami, A momentum-based balance controller for humanoid robots on non-level and non-stationary ground, Autonomous Robots, 33(4):399–414, Springer, 2012.
[14] A. Macchietto, V. Zordan and C. R. Shelton, Momentum control for balance, ACM Trans. Graphics, 28(3):80–87, 2009.
[15] D. W. Marhefka and D. E. Orin, A compliant contact model with nonlinear damping for simulation of robotic systems, IEEE Trans. Systems, Man, and Cybernetics-part A: Systems and Humans, 29(6):566–572, 1999.
[16] N. Xydes and I. Kao, Modeling of contact mechanics and friction limit surfaces for soft fingers in robotics, with experimental results, Int. J. Robotics Research, 18(9):941–950, Sep 1999.
[17] http://royfeatherstone.org/spatial/v2/index.html

4.3 Making use of reasonable rigidity assumptions

However, estimating z with high bandwith and precision is a very complex problem and relying on such an assumption is doomed to fail.

References

[1] O. Khatib, L. Sentis, and J.-H. Park, "A unified framework for whole-body humanoid robot control with multiple constraints and contacts," in *European Robotics Symposium 2008*, ser. Springer Tracts in Advanced Robotics. Springer Berlin / Heidelberg, 2008, vol. 44, pp. 303–312.

[2] L. Sentis, J. Park, and O. Khatib, "Compliant control of multi-contact and center of mass behaviors in humanoid robots," *IEEE Transactions on Robotics*, vol. 26, no. 3, pp. 483–501, june 2010.

[3] L. Righetti, J. Buchli, M. Mistry, M. Kalakrishnan, and S. Schaal, "Optimal distribution of contact forces with inverse dynamics control," *The International Journal of Robotics Research*, 2013.

[4] Y. Abe, M. da Silva, and J. Popović, "Multiobjective control with frictional contacts," in *Proceedings of the ACM SIGGRAPH/Eurographics symposium on Computer animation*, 2007, pp. 249–258.

[5] M. Liu, A. Micaelli, P. Evrard, A. Escande, and C. Andriot, "Interactive dynamics and balance of a virtual character during manipulation tasks," in *IEEE International Conference on Robotics and Automation (ICRA)*, may 2011, pp. 1676–1682.

[6] J. Salini, V. Padois, and P. Bidaud, "Synthesis of complex humanoid whole-body behavior: A focus on sequencing and tasks transitions," in *IEEE International Conference on Robotics and Automation*, may 2011, pp. 1283 –1290.

[7] J. Salini, S. Barthlemy, P. Bidaud, and V. Padois, "Whole-body motion synthesis with lqp-based controller - application to icub," in *Cognitive Systems Monographs : Modeling, Simulation and Optimization of Bipedal Walking*, K. Mombaur and K. Berns, Eds. Springer Berlin Heidelberg, 2013, vol. 18, pp. 119–210.

[8] L. Saab, O. Ramos, F. Keith, N. Mansard, P. Soueres, and J.-Y. Fourquet, "Dynamic whole-body motion generation under rigid contacts and other unilateral constraints," *Robotics, IEEE Transactions on*, vol. 29, no. 2, pp. 346–362, 2013.

[9] B. Stephens and C. Atkeson, "Dynamic balance force control for compliant humanoid robots," in *IEEE/RSJ International Conference on Intelligent Robots and Systems (IROS)*, oct. 2010, pp. 1248–1255.

[10] F. Nori, S. Traversaro, J. Eljaik, F. Romano, A. Del Prete, and D. Pucci, "icub whole-body control through force regulation on rigid noncoplanar contacts," *Frontiers in Robotics and AI*, 2015.

[11] U. Muico, Y. Lee, J. Popović, and Z. Popović, "Contact-aware nonlinear control of dynamic characters," *ACM Trans. Graph.*, vol. 28, pp. 81:1–81:9, July 2009.

[12] O. Khatib, "A unified approach for motion and force control of robot manipulators: The operational space formulation," *Robotics and Automation, IEEE Journal of*, vol. 3, no. 1, pp. 43–53, 1987.

[13] N. Hogan, "Impedance control: An approach to manipulation - part i: Theory; part ii: Implementation; part iii: Applications," *Journal of dynamic systems, measurement, and control*, vol. 107, no. 1, pp. 1–24, 1985.

[14] L. Love and W. Book, "Environment estimation for enhanced impedance control," in *IEEE International Conference on Robotics and Automation*, vol. 2, May 1995, pp. 1854–1859 vol.2.

[15] T. Tsumugiwa, R. Yokogawa, and K. Hara, "Variable impedance control based on estimation of human arm stiffness for human-robot cooperative calligraphic task," in *IEEE International Conference on Robotics and Automation*, vol. 1, 2002, pp. 644–650 vol.1.

[16] J. Buchli, E. Theodorou, F. Stulp, and S. Schaal, "Variable impedance control-a reinforcement learning approach." in *Robotics: Science and Systems*, 2010.

[17] C. Yang, G. Ganesh, S. Haddadin, S. Parusel, A. Albu-Schaeffer, and E. Burdet, "Human-like adaptation of force and impedance in stable and unstable interactions," *IEEE Transactions on Robotics*, vol. 27, no. 5, pp. 918–930, Oct 2011.

[18] K. Bouyarmane and A. Kheddar, "Fem-based static posture planning for a humanoid robot on deformable contact support," in *Proceedings of the 11th IEEE-RAS International Conference on Humanoid Robots*, Oct 2011, pp. 487–492.

[19] N. Xydes and I. Kao, "Modeling of contact mechanics and friction limit surfaces for soft fingers in robotics, with experimental results," *Int. J. Robotics Research*, vol. 18, no. 9, pp. 941–950, Sep 1999.

[20] S. Jain and C. Liu, "Controlling physics-based characters using soft contacts," *ACM Trans. Graphics*, vol. 30, no. 6, 2011.

[21] J. Salini, V. Padois, and P. Bidaud, "Synthesis of complex humanoid whole-body behavior: a focus on sequencing and tasks transitions," in *Proceedings of the IEEE International Conference on Robotics and Automation*, 2011, pp. 1283–1290.

[22] K. Bouyarmane and A. Kheddar, "Using a multi-objective controller to synthesize simulated humanoid robot motion with changing contact configurations," in *Proceedings of the IEEE/RSJ International Conference on Intelligent Robots and Systems*. IEEE, 2011, pp. 4414–4419.

[23] A. Herzog, L. Righetti, F. Grimminger, P. Pastor, and S. Schaal, "Balancing experiments on a torque-controlled humanoid with hierarchical inverse dynamics," in *Intelligent Robots and Systems (IROS 2014), 2014 IEEE/RSJ International Conference on*. IEEE, 2014, pp. 981–988.

[24] A. Escande, N. Mansard, and P.-B. Wieber, "Hierarchical quadratic programming: Fast online humanoid-robot motion generation," *The International Journal of Robotics Research*, p. 0278364914521306, 2014.

[25] M. Liu, Y. Tan, and V. Padois, "Generalized hierarchical control," *Autonomous Robots*, vol. 40, no. 1, pp. 17–31, 2016.

[26] M. Liu, R. Lober, and V. Padois, "Whole-body hierarchical motion and force control for humanoid robots," *Autonomous Robots*, vol. 40, no. 3, pp. 493–504, 2016.

[27] S. Lee and A. Goswami, "A momentum-based balance controller for humanoid robots on non-level and non-stationary ground," *Autonomous Robots*, vol. 33, no. 4, pp. 399–414, 2012.

[28] N. Perrin, D. Lau, and V. Padois, "Effective generation of dynamically balanced locomotion with multiple non-coplanar contacts," in *Proceedings of the International Symposium on Robotics Research*, Sestri Levante, Italy, Sep. 2015.

[29] A. Herzog, N. Rotella, S. Mason, F. Grimminger, S. Schaal, and L. Righetti, "Momentum control with hierarchical inverse dynamics on a torque-controlled humanoid," *Autonomous Robots*, vol. 40, no. 3, pp. 473–491, 2015. [Online]. Available: http://dx.doi.org/10.1007/s10514-015-9476-6

[30] M. Liu and V. Padois, "Reactive whole-body control for humanoid balancing on non-rigid unilateral contacts," in *Proceedings of the IEEE/RSJ International Conference on Intelligent Robots and Systems*, Hamburg, Germany, Sep. 2015, pp. 3981–3987.

[31] M. Azad and M. N. Mistry, "Balance control strategy for legged robots with compliant contacts," in *Proceedings of the IEEE International Conference on Robotics and Automation*, May 2015, pp. 4391–4396.

[32] H. Dallali, M. Mosadeghzad, G. Medrano-Cerda, and N. Docquier, "Development of a dynamic simulator for a compliant humanoid robot based on a symbolic multibody approach," in *Proceedings of the IEEE International Conference on Mechatronics*, Vicenza, Italy, Feb 2013, pp. 598–603.

[33] N. Diolaiti, C. Melchiorri, and S. Stramigioli, "Contact impedance estimation for robotic systems," *IEEE Trans. Robotics*, vol. 21, no. 5, pp. 925–935, Oct 2005.

[34] D. Erickson, M. Weber, and I. Sharf, "Contact stiffness and damping estimation for robotic systems," *Int. J. Robotics Research*, vol. 22, no. 1, pp. 41–57, Jan 2003.